Biochimica et Biophysica Acta 1827 (2013) 94–113

Contents lists available at SciVerse ScienceDirect

Biochimica et Biophysica Acta

journal homepage: www.elsevier.com/locate/bbabio

Review

Energy conservation via electron bifurcating ferredoxin reduction and proton/Na^+ translocating ferredoxin oxidation ☆

Wolfgang Buckel *, Rudolf K. Thauer

Max-Planck-Institut für terrestrische Mikrobiologie, Karl-von-Frisch-Str. 10, 35043 Marburg, and Fachbereich Biologie, Philipps-Universität, Marburg, Germany

ARTICLE INFO

Article history:
Received 9 May 2012
Received in revised form 5 July 2012
Accepted 7 July 2012
Available online 16 July 2012

Keywords:
Flavin-based electron bifurcation (FBEB)
Flavin semiquinone
Etf-Butyryl-CoA Dehydrogenase Complex
[FeFe] and [FeNi]hydrogenases
NADH:NADPH Transhydrogenase
Heterodisulfide Reductase Complex

ABSTRACT

The review describes four flavin-containing cytoplasmatic multienzyme complexes from anaerobic bacteria and archaea that catalyze the reduction of the low potential ferredoxin by electron donors with higher potentials, such as NAD(P)H or H_2 at ≤100 kPa. These endergonic reactions are driven by concomitant oxidation of the same donor with higher potential acceptors such as crotonyl-CoA, NAD^+ or heterodisulfide (CoM-S-S-CoB). The process called flavin-based electron bifurcation (FBEB) can be regarded as a third mode of energy conservation in addition to substrate level phosphorylation (SLP) and electron transport phosphorylation (ETP). FBEB has been detected in the clostridial butyryl-CoA dehydrogenase/electron transferring flavoprotein complex (BcdA-EtfBC), the multisubunit [FeFe]hydrogenase from *Thermotoga maritima* (HydABC) and from acetogenic bacteria, the [NiFe]hydrogenase/heterodisulfide reductase (MvhADG–HdrABC) from methanogenic archaea, and the transhydrogenase (NfnAB) from many Gram positive and Gram negative bacteria and from anaerobic archaea.

The Bcd/EtfBC complex that catalyzes electron bifurcation from NADH to the low potential ferredoxin and to the high potential crotonyl-CoA has already been studied in some detail. The bifurcating protein most likely is EtfBC, which in each subunit (βγ) contains one FAD. In analogy to the bifurcating complex III of the mitochondrial respiratory chain and with the help of the structure of the human ETF, we propose a conformational change by which γ-$FADH^-$ in EtfBC approaches β-FAD to enable the bifurcating one-electron transfer. The ferredoxin reduced in one of the four electron bifurcating reactions can regenerate H_2 or NADPH, reduce CO_2 in acetogenic bacteria and methanogenic archaea, or is converted to $\Delta\mu H^+/Na^+$ by the membrane-associated enzyme complexes Rnf and Ech, whereby NADH and H_2 are recycled, respectively. The mainly bacterial Rnf complexes couple ferredoxin oxidation by NAD^+ with proton/sodium ion translocation and the more diverse *e*nergy *c*onverting [NiFe]*h*ydrogenases (Ech) do the same, whereby NAD^+ is replaced by H^+. Many organisms also use Rnf and Ech in the reverse direction to reduce ferredoxin driven by $\Delta\mu H^+/Na^+$. Finally examples are shown, in which the four bifurcating multienzyme complexes alone or together with Rnf and Ech are integrated into energy metabolisms of nine anaerobes. This article is part of a Special Issue entitled: The evolutionary aspects of bioenergetic systems.

1. Introduction

The electron carrier ferredoxin is involved in the energy metabolism of many anaerobes e.g. clostridia, acetogenic and sulfate reducing bacteria as well as methanogenic archaea. Ferredoxins are cytoplasmic, acidic iron–sulfur proteins with either one [2Fe–2S] cluster or one, two or more [4Fe–4S] clusters each of which can be reduced by one electron. The redox potentials $E^{o'}$ of ferredoxins are close to that of the hydrogen (H_2) electrode at pH 7.0 which is −414 mV. This reflects that in most energy metabolisms, in which ferredoxins are involved, dihydrogen is either a substrate or a product. Within the cells the ferredoxins are more than 90% reduced allowing them to serve as electron donors in reactions with standard redox potentials ($E^{o'}$) as low as or even below −500 mV. Under conditions of iron deprivation many anaerobes synthesize flavodoxins instead of ferredoxins and the flavodoxins substitute for the ferredoxins in most functions (Table 1) [1–5].

Until recently the following catabolic ferredoxin-dependent redox reactions were known, some of which can function in vivo in both directions (not complete): the reduction of protons to H_2 ($E^{o'} = -414$ mV) [14], the reversible oxidation of pyruvate to acetyl-CoA and CO_2 ($E^{o'} = -500$ mV) [15], the reversible oxidation of CO to CO_2 ($E^{o'} = -520$ mV) [16], the reversible oxidation of formyl-methanofuran to

☆ This article is part of a Special Issue entitled: The evolutionary aspects of bioenergetic systems.

* Corresponding author. Tel.: +49 6421 2822088; fax: +49 6421 2828979.
E-mail addresses: buckel@staff.uni-marburg.de, buckel@biologie.uni-marburg.de (W. Buckel).

0005-2728/$ – see front matter © 2012 Elsevier B.V. All rights reserved.
doi:10.1016/j.bbabio.2012.07.002

CO_2 and methanofuran ($E^{o'} = -500$ mV) [12], the oxidation of acetaldehyde to acetic acid ($E^{o'} = -580$ mV) [17], the reversible oxidation of formate to CO_2 ($E^{o'} = -430$ mV) [18] and the oxidation of 3-phosphoglyceraldehyde to 3-phosphoglycerate ($E^{o'} = -580$ mV) [19]. These reactions are catalyzed by cytoplasmic iron–sulfur proteins some of which additionally contain thiamine pyrophosphate (pyruvate: ferredoxin oxidoreductase), nickel (CO dehydrogenase) or molybdopterin coordinating molybdenum or tungsten (formylmethanofuran dehydrogenase, acetaldehyde: ferredoxin oxidoreductase, formate: ferredoxin oxidoreductase and 3-phosphoglyceraldehyde: ferredoxin oxidoreductase). In addition reduced ferredoxin acts as electron donor for nitrogen fixation [20], activation of (*R*)-2-hydroxyacyl-CoA dehydratases [21], and reduction of benzoyl-CoA by the ATP-dependent [22] and independent enzyme systems (see Section 2.5).

In an energy metabolism for every ferredoxin-reducing reaction there must be at least one ferredoxin oxidizing reaction and these reactions must be stoichiometrically balanced. However, this was not always found to be the case, indicating that our knowledge with respect to ferredoxin-dependent reactions was not complete. Thus in the energy metabolism of *Clostrium kluyveri* growing on ethanol and acetate, H_2 is formed in a ferredoxin-dependent reaction but there was no reaction known that can regenerate the reduced ferredoxin in vivo [11]. It was also not known, whether the free energy change associated with the re-oxidation of reduced ferredoxin with NAD^+ or protons can be conserved. Both questions have in the meantime been resolved.

In the last few years two novel types of ferredoxin-dependent catabolic enzymes were found: (i) the cytoplasmic enzyme complexes coupling the endergonic reduction of ferredoxin with NADH, NADPH or H_2 to exergonic redox reactions via flavin-based electron bifurcation; and (ii) the membrane associated complexes RnfA–G and the energy converting [NiFe]hydrogenase complex catalyzing the reversible oxidation of reduced ferredoxin with NAD^+ and H^+, respectively, and coupling these exergonic reactions with the build-up of an electrochemical proton or sodium ion potential.

Flavin-based electron bifurcation was first proposed by Herrmann et al. [23] in analogy to ubiquinone based electron bifurcation in mitochondria, in which the exergonic one-electron oxidation of the fully reduced ubiquinol by the Rieske [2Fe–2S] cluster triggers the one-electron reduction of cytochrome *b* by the ubisemiquinone radical [24]. It was proposed that similar exergonic one-electron oxidations of fully reduced flavins in some flavoproteins could trigger the formation of a flavin semiquinone radical with a redox potential sufficiently negative to allow the reduction of ferredoxins.

The review deals first with the structure and properties of the cytoplasmic ferredoxin-dependent enzyme complexes coupling endergonic and exergonic redox reactions. This is followed by a section on the structure and properties of the membrane-associated membrane complexes catalyzing the reversible oxidation of reduced ferredoxin. Sections 2 and 3 are summarized in Table 2. In a third section the function of the novel ferredoxin-dependent enzyme complexes in the energy metabolism is exemplarily described. Finally, it is discussed, whether there could be other electron bifurcating systems not based on flavins in anaerobic microorganisms.

2. Cytoplasmic enzyme complexes coupling endergonic ferredoxin reduction reactions to exergonic redox reactions presumably via flavin-based electron bifurcation

In 2008 it was shown for the first time that in *C. kluyveri* the endergonic reduction of ferredoxin with NADH is coupled to the exergonic reduction of crotonyl-CoA to butyryl-CoA (Reaction (1)) and that this coupled reaction is catalyzed by a cytoplasmic enzyme complex [25]. Since then three more such coupled reactions catalyzed by cytoplasmic protein complexes were discovered (Reactions (2)–(4)) [26–28]. And this appears to be just the tip of an iceberg. Candidates for coupled reactions are the reduction of methylenetetrahydrofolate to methyltetrahydrofolate in acetogenic bacteria, the reduction of benzoyl-CoA in energy-limited anaerobic bacteria, the oxidation of formate in *Clostridium acidi-urici*, and the reduction of adenosine phosphosulfate (APS) as will be outlined in Section 2.5.

$$Fd_{ox} + 2NADH + \text{crotonyl–CoA} \rightarrow Fd^{2-}_{red} + 2NAD^+ + \text{butyryl–CoA} \quad (1)$$
$$\Delta G^o = -44\,kJ/mol$$

$$Fd_{ox} + 2H_2 + NAD^+ \rightleftharpoons Fd^{2-}_{red} + NADH + 3H^+ \quad (2)$$
$$\Delta G^o = -21\,kJ/mol$$

$$Fd_{ox} + 2H_2 + \text{CoM–S–S–CoB} \rightarrow Fd^{2-}_{red} + \text{CoM–SH} + \text{CoB–SH} + 2H^+ \quad (3)$$
$$\Delta G^o = -50\,kJ/mol$$

Table 1
Redox potentials of cofactors or substrates mentioned in this article.

Oxidized cofactor/substrate	Reaction	$E^{o'}$ (standard conditions)	E' (physiological conditions)
Ferredoxin (Fd, clostridial type)[a] [4,5]	$Fd + e^- = Fd^-$	ca. −400 mV	ca. −500 mV
	$Fd^- + e^- = Fd^{2-}$	ca. −400 mV	ca. −500 mV
NAD^+ [6]	$NAD^+ + 2\,e^- + H^+ = NADH$	−320 mV	−280 mV
$NADP^+$ [6]	$NADP^+ + 2\,e^- + H^+ = NADPH$	−320 mV	−380 mV
FAD (or FMN) [7]	$FAD + e^- (+H^+) = FAD(H)^{\bullet}(^-)$	−172 mV	Variable[b]
	$FAD(H)^{\bullet}(^-) + e^- (+H^+) = FADH^-$	−238 mV	Variable
	$FAD + 2e^- + H^+ = FADH^-$	−205 mV	Variable
Flavodoxin (Fld) [8]	$Fld + e^- + H^+ = FldH^{\bullet}$	−60 mV	
	$FldH^{\bullet} + e^- = FldH^-$	−420 mV	
ETF (porcine) [9]	$ETF + e^- = ETF^{\bullet -}$	+4 ± 15 mV	
	$ETF^{\bullet -} + e^- + H^+ = ETFH^-$	−50 ± 16 mV	
	$ETF + 2\,e^- + H^+ = ETFH^-$	−23 mV	
Crotonyl-CoA [10]	$\text{Crotonyl-CoA} + 2\,H^+ + 2\,e^- = \text{butyryl-CoA}$	−10 mV	
H^+/H_2 [11]	$2\,H^+ + 2\,e^- = H_2$	−414 mV	≤ −296 mV (≥10 Pa H_2)
CO_2/CO [11]	$CO_2 + 2\,H^+ + 2\,e^- = CO + H_2O$	−520 mV	
CO_2/formate [11]	$CO_2 + H^+ + 2\,e^- = HCO_2^-$	−420 mV	
CO_2/methanofuran (MFH) [12]	$CO_2 + MFH + 2\,H^+ + 2\,e^- = \text{Formyl-MF} + H_2O$	−500 mV	
CO_2/pyruvate [11]	$CO_2 + \text{Acetyl-CoA} + H^+ + 2\,e^- = \text{Pyruvate}^- + \text{CoA-SH}$	−500 mV	
Heterodisulfide, CoM-S-S-CoB [13]	$\text{CoM-S-S-CoB} + 2\,H^+ + 2\,e^- = \text{CoM-SH} + \text{CoB-SH}$	−140 mV	

[a] The redox potentials of ferredoxins from different clostridia slightly vary.
[b] Binding of flavins to proteins strongly influences their E', see e.g. Fld and ETF.

$$Fd_{ox} + 2NADPH + NAD^+ \rightleftharpoons Fd^{2-}_{red} + NADH + 2NADP^+ + H^+ \quad (4)$$

$$\Delta G^o = +16 kJ/mol.$$

Fd in Reactions (1)–(4) is the abbreviation for ferredoxin. Fd from *C. pasteurianum*, which was used in most of the experiments, has a molecular mass of 6 kDa and a pI of 3.7 [1]. It contains two [4Fe–4S] clusters both with a midpoint redox potential of near −400 mV [4] and this is the redox potential $E^{o'}$ used in the calculations of the free energy changes ($\Delta G^{o'}$) associated with Reactions (1) to (4). The ferredoxins from *Acidaminococcus fermentans* and *Clostridium tetanomorphum* have similar properties. Also used were $E^{o'} = -320$ mV for the NAD^+/NADH couple, $E^{o'} = -320$ mV for the $NADP^+$/NADPH couple, $E^{o'} = -10$ mV for the crotonyl-CoA/butyryl-CoA couple [10] and $E^{o'} = -140$ mV for the CoM-S-S-CoB/CoM-SH + CoB-SH couple (Table 1) [29].

For the understanding of the thermodynamics of Reactions (1) to (4) it is important to know that in living cells ferredoxins are generally more than 90% reduced ($E' = -500$ mV), that NAD is more than 90% oxidized ($E' = -280$ mV) and that the $NADP^+$/NADPH ratio is 1/40 ($E' = -360$ mV) [6]. Thus transhydrogenation from NADH ($E' = -280$ mV) to $NADP^+$ ($E' = -360$ mV) in living cells requires energy [30] as does the reduction of ferredoxin ($E' = -500$ mV) with H_2 at 10 Pa ($E' = -300$ mV), which is the H_2 partial pressure in methanogenic habitats [29]. The redox potential E' of the Fd_{ox}/Fd^{2-}_{red} couple was set at −500 mV because this is the redox potential at which in anaerobes many ferredoxin-dependent reactions operate. Examples are the pyruvate:ferredoxin oxidoreductase reaction ($E^{o'} = -500$ mV) [11], the CO dehydrogenase reaction ($E^{o'} = -520$ mV) [11] and the formylmethanofurane dehydrogenase reaction ($E^{o'} = -500$ mV) [29].

The cytoplasmic enzyme complexes catalyzing Reactions (1)–(4) contain FAD or FMN. The butyryl-CoA dehydrogenase/electron transferring flavoprotein complex (BcdA–EtfBC complex) catalyzing Reaction (1) contains four FAD and no other prosthetic group. This is at present the strongest argument why we think that coupling of the endergonic reduction of ferredoxin with NADH, NADPH or H_2 is via flavin-based electron bifurcation in analogy to ubiquinone-based electron bifurcation discussed in Section 2.6. The [FeFe]hydrogenase complex HydABC (Reaction (2)), the [NiFe]hydrogenase–heterodisulfide reductase complex MvhADG/HdrABC (Reaction (3)) and the transhydrogenase complex NfnAB (Reaction (4)) contain besides FAD (HdrA and NfnAB) or FMN (HydAB) also many iron–sulfur clusters. They most likely have a function in electron transport but could equally well store electrons. Also, an iron sulfur cluster-based electron bifurcation mechanism, although not very likely, has to be considered. HydABC and NfnAB catalyze reversible reactions. They are electron confurcating rather than electron bifurcating when catalyzing the oxidation of reduced ferredoxin.

2.1. BcdA–EtfBC complex coupling ferredoxin reduction with NADH to crotonyl-CoA reduction

In 1971 it was reported that cell extracts from *C. kluyveri* catalyzed the reduction of ferredoxin with NADH only in the presence of acetyl-CoA and that concomitant to ferredoxin also acetyl-CoA was reduced [31,32]. The results were interpreted to indicate that the cell extracts contained an enzyme that catalyzes the reduction of ferredoxin with NADH under the allosteric control of the acetyl-CoA/CoA couple. The reduction of acetyl-CoA was thought to be catalyzed by separate enzymes. Forty years later evidence was presented that these activities all belong to one enzyme, namely the butyryl-CoA dehydrogenase-EtfBC complex (BcdA–EtfBC) catalyzing Reaction (1) (see also Section 4.3) [23,25].

A BcdA–EtfBC complex (Fig. 1) capable of catalyzing Reaction (1) was first purified from *C. kluyveri* by using the standard acyl-CoA dehydrogenase assay with butyryl-CoA and ferricenium

Table 2
Properties of enzymes mentioned in this article.

Enzyme	Abbreviation	Source	Subunits	Prosthetic groups
Bct/Etf complex	BctA–EtfBC	*Clostridium kluyveri* *C. tetanomorphum*	$(BcdA–EtfBC)_2$ heterohexamer?	4(?) FAD
Butyryl-CoA dehydrogenase	BcdA	*Acidaminococcus fermentans*	$(BcdA)_4$	4 FAD
Electron transferring flavoprotein	EtfBC	*A. fermentans*	EtfBC	2 FAD
Electron transferring flavoprotein	ETF; EtfBC	Human	EtfB	FAD
			EtfC	AMP
Bifurcating hydrogenase	HydABC	*Thermotoga maritima*, acetogenic bacteria	HydA	[FeFe]hydrogenase 3[4Fe–4Fe], [2Fe–2Fe]
			HydB	3[4Fe–4Fe], [2Fe–2Fe] 2 FMN?
			HydC	[2Fe–2Fe]
Hydrogenase-heterodisulfide reductase	MvhADG–HdrABC	*Methanothermobacter marburgensis*, other methanogens	MvhA	[NiFe]hydrogenase 2 [4Fe–4Fe], [3Fe–4Fe]
			MvhD	[2Fe–2Fe]
			MvhG	2 [4Fe–4Fe], [3Fe–4Fe]
			HdrA	FAD, 4 [4Fe–4Fe]
			HdrB	2 [4Fe–4Fe]
			HdrC	Zn^{2+}, [4Fe–4Fe]
Trans-hydrogenase	NfnAB	*C. kluyveri*, many anaerobic bacteria	NfnA	FAD, [2Fe–2Fe]
			NfnB	2 [4Fe–4Fe]
NAD-ferredoxin reductase	Rnf;RnfABCDEG	*C. tetanomorphum*, many anaerobic bacteria, *Methanosarcina*	RnfADE	Transmembrane proteins
			RnfB	4 [4Fe–4Fe], [3Fe–4Fe]
			RnfC	FMN, 2 [4Fe–4Fe]
			RnfD	covalent FMN, riboflavin
			RnfG	covalent FMN
Energy converting [NiFe] hydrogenase	Ech; EchABCDEF	*Rhodospirillum rubrum*, *Carboxidothermus hydrogenoformans*, archaea and others	EchAB	Transmembrane proteins
			EchC	[4Fe–4Fe]
			EchD	None
			EchE	[NiFe]hydrogenase
			EchF	2 [4Fe–4Fe]

hexafluorophosphate as electron acceptor. With partially purified fractions the 'bifurcation assay' could be applied. The assay comprised crotonyl-CoA, NADH and the enzyme source. NADH oxidation was only observed after addition of catalytic amounts of ferredoxin (Eq. (1)) and the cytoplasmic monomeric [FeFe]hydrogenase from *C. pasteurianum* [33]; the latter was necessary to regenerate oxidized ferredoxin resulting in formation of molecular hydrogen (Eq. (5)).

$$Fd_{ox} + 2NADH + \text{crotonyl–CoA} \rightarrow Fd_{red}^{2-} + 2NAD^{+} + \text{butyryl–CoA} \quad (1)$$

$$Fd_{red}^{2-} + 2H^{+} \rightarrow Fd_{ox} + H_2 \quad (5)$$

$$\text{Crotonyl–CoA} + 2NADH + 2H^{+} \rightarrow \text{butyryl–CoA} + 2NAD^{+} + H_2. \quad (1+5)$$

Purification of the BcdA–EtfBC complex was performed under strictly anoxic conditions and in the presence of FAD; otherwise the activity was rapidly lost. The molecular masses of the subunits determined by SDS-PAGE were: α (Bcd) 41 kDa, β (EtfB) 36 kDa and γ (EtfC) 28 kDa. A photometric scan of an SDS-PAGE run stained with Coomassie brilliant blue yielded a stoichiometry of 1.8:1:1. Gel filtration on Superdex 200 revealed 320 kDa, which matches with 292 kDa, the sum of the subunit molecular masses indicating a quaternary structure of $\alpha_4\beta_2\gamma_2$ (Fig. 1). N-Terminal sequencing of the three subunits detected the corresponding gene cluster in the *C. kluyveri* genome: *bcdA* (CKL_0455), *etfC* (CKL_0456) and *etfB* (CKL_0457) [25]. The genome contains an additional *bcdA-etfBC* cluster which apparently is not expressed under growth on ethanol and acetate [34].

During purification of the BcdA–EtfBC complex inactive fractions were detected, which either contained BcdA or EtfBC alone. Hence the complex appeared to dissociate under certain conditions, but whether the recombined fractions regained activity was not tested. Although the amount of FAD in the BcdA–EtfBC complex was not analyzed, it can be assumed that each subunit of the $\alpha_4\beta_2\gamma_2$ complex contains one molecule of this cofactor. This is based on the structures of acyl-CoA dehydrogenases and EtfBC from *Megasphaera elesdenii*, formerly called *Peptostreptococcus elsdenii*, the only well-studied Etf from a strictly anaerobic bacterium [35,36].

A BcdA–EtfBC complex structurally and functionally almost identical to that from *C. kluyveri* was isolated from *C. tetanomorphum* with subunits as determined by SDS-PAGE: α (Bcd) 40 kDa, β (EtfB) 36 kDa and γ (EtfC) 28 kDa. The apparent molecular mass of the whole complex determined as 574 kDa by size exclusion chromatography is exactly twice as high as that calculated for the expected $\alpha_4\beta_2\gamma_2$ composition (288 kDa); hence the complex most likely has an $(\alpha_2\beta\gamma)_4$ composition [37–39].

In *A. fermentans* (see also Section 4.4) the yellow EtfBC and the green butyryl-CoA dehydrogenase were isolated as separate molecules. Their activities were detected by diaphorase (NADH + iodonitrosotetrazolium chloride) and ferricenium assays, respectively. This EtfBC exhibited a FAD-content of 0.5 mol/heterodimer, which increased to 2 mol upon incubation with FAD and removal of the excess by gel filtration (A. M. Mowafy, Z. Li, and W. Buckel, unpublished).

The BcdA–EtfBC complexes from *C. kluyveri* and from *C. tetanomorphum* as well as a 1:1 mixture of Bcd and EtfBC from *A. fermentans* catalyzed the bifurcation reaction according to Eq. (1 + 5). The formed hydrogen was measured by gas chromatography (0.7 H_2/crotonyl-CoA) and the stoichiometry of NADH oxidation was determined as 1.8 ± 0.2 NADH/crotonyl-CoA. Alternatively, oxidized ferredoxin was regenerated with partially purified membrane associated NAD-ferredoxin oxidoreductase from *C. tetanomorphum* also called Rnf (Eq. (6); see Section 3.1.) resulting in Eq. (1 + 6). Due to the presence of detergent in vitro, no $\Delta\mu Na^{+}$ could be observed. In vivo,

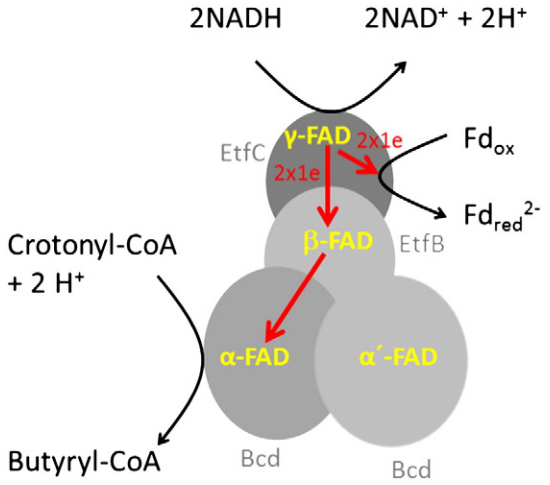

Fig. 1. Schematic representation of the structure and function of the clostridial BcdA–EtfBC complex. Only half of the calculated $\alpha_4\beta_2\gamma_2$-structure is shown. The interaction of NADH, ferredoxin (Fd) and Bcd with Etf is arbitrarily assumed.

however, Eq. (1 + 6) represents an anaerobic respiratory chain as will be outlined in Section 4 [38].

$$Fd_{red}^{2-} + NAD^{+} + H^{+} = Fd_{ox} + NADH + (\Delta\mu Na^{+}/H^{+}); \quad (6)$$

$$Fd_{ox} + 2NADH + \text{crotonyl–CoA} \rightarrow Fd_{red}^{2-} + 2NAD^{+} + \text{butyryl–CoA}; \quad (1)$$

$$\text{Crotonyl–CoA} + NADH + H^{+} = \text{butyryl–CoA} + NAD^{+} + (\Delta\mu Na^{+}/H^{+}). \quad (1+6)$$

The electron transferring flavoproteins (ETF) are defined as heterodimeric FAD containing proteins mediating electron transport between a dehydrogenase and an ETF-quinone oxidoreductase. The ETFs from clostridia form a special group, which together with an acyl-CoA dehydrogenase catalyze in part the reverse reaction, the reduction of enoyl-CoA by NADH. The mammalian ETF was discovered in 1956 by F. L. Crane and Helmut Beinert as a yellow protein that carries one electron from the usually green acyl-CoA dehydrogenases in the mitochondrial matrix to the inner membrane, where it becomes re-oxidized by ubiquinone (Q) mediated by ETF–Q oxidoreductase (Reactions (7) and (8)) [40]. The FAD-containing mainly tetrameric acyl-CoA dehydrogenases (α_4) catalyzes the first step of the β-oxidation, the reversible dehydrogenation of acyl-CoA to (*E*)-2-enoyl-CoA [41]. ETF is a heterodimeric protein (βγ; human ETF: β, 40 kDa; γ 30 kDa) that contains one FAD in the β-subunit and one AMP in the γ-subunit. The crystal structure of the human ETF (Fig. 2) can be subdivided into three domains [42]. Domains I (amino acids 1–205) and II (206–331) stem from the β-subunit, whereas the γ-subunit provides domain III (1–220) and a more than 50 Å long C-terminal arm (221–262) that wraps around domains I and II. The structures of domains I and III are highly related which is already reflected in significant similarities of their primary structures. Presumably, subunits β and γ have evolved from a common ancestor by a gene duplication event. Domains I and III are multiply connected by an extended contact area and constitute a compact core. Domain II is only loosely attached to this core mainly via the mentioned C-terminal arm of the γ-subunit. This architecture of ETF allows conformational changes of domain II relative to the core either induced by NADH or other proteins. FAD is located in a stretched conformation on the surface of domain II with the isoalloxazine ring pointing toward AMP that is embedded into the center of domain III. Hence the distance between AMP and FAD could decrease when domain II moves toward domains I + III. Modeling and cross-linking studies support an interaction of the acyl-CoA dehydrogenase with

ETF between domains II and III, which would be the shortest possible distance for an electron transfer between both FADs [42].

It has been shown that ETF shuttles only one electron from the dehydrogenase to the oxidoreductase (Reactions (7) and (8)). Thus ETF is able to stabilize the red semiquinone anion ($ETF^{\bullet -}$) [43]. This is structurally supported by the flavodoxin fold of domain II [42] and by a hydrogen bond between 4′-OH of the ribityl side chain and N(1) of the isoalloxazine ring [44].

$$\text{Acyl–CoA dehydrogenase} : \text{Acyl–CoA} + 2\text{ETF} \rightarrow \text{Enoyl–CoA} + 2\text{ETF}^{\bullet -} + 2\text{H}^{+} \quad (7)$$

$$\text{ETF–Q coxidoreductase} : 2\text{ETF}^{\bullet -} + 2\text{H}^{+} + \text{Q} \rightarrow 2\text{ETF} + \text{QH}_2. \quad (8)$$

The human type ETF is not only wide-spread among animals but also common in aerobic bacteria, which thrive on the oxidation of fatty acids [45]. The high sequence identities between the human type ETFs and the bifurcating EtfBCs suggest that also the crystal structures are similar. The only difference is that the latter interact with NADH, whereas the human type ETF and the acyl-CoA dehydrogenases do not. This corroborates with the presence of the second FAD molecule in EtfBCs of *A. fermentans* and *M. elsdenii*, which probably replaces the AMP.

Assuming that all bifurcating EtfBCs contain two FAD, one in each subunit, we propose following hypothetical mechanism, modified after [46] (Fig. 3). NADH reduces γ-FAD (FAD in the γ-subunit) to γ-$FADH^{-}$, which due to the unfavorable redox potentials cannot transfer one electron further to ferredoxin. However, β-FAD sitting in the flavodoxin domain of the β-subunit could swing over to γ-$FADH^{-}$ and get one electron to become β-$FAD^{\bullet -}$, which swings back before the next electron can follow. Similar to flavodoxin, domain II should be able to stabilize the semiquinone anion. The remaining electron on the now formed semiquinone γ-FADH• is not stabilized by the protein and highly reactive ("red hot") to immediately reduce ferredoxin (Fd) to Fd^{-} [47]. The stabilized semiquinone anion β-$FAD^{\bullet -}$ transfers the electron further to Bcd where it is stored. Then another NADH enters EtfBC starting a next bifurcation by which Fd^{-} is further reduced to Fd^{2-} and Bcd gets the second electron to convert crotonyl-CoA to butyryl-CoA. A conformational change similar to that postulated in this mechanism has been identified for the Rieske [2Fe–2S] cluster in the bifurcating cytochrome bc_1 complex (see Section 2.6). An alternative "thermodynamic mechanism" is proposed in Section 2.4.

2.2. HydABC complex coupling reversible ferredoxin reduction with H_2 to NAD^+ reduction

The second cytoplasmic enzyme complex with an electron bifurcation coupling mechanism was discovered by Schut and Adams in 2009 [26]. They could show that the heterotrimeric [FeFe]hydrogenase from *Thermotoga maritima* [48], which is rapidly inactivated in the presence of even trace amounts of oxygen, catalyzes the formation of H_2 with reduced ferredoxin as electron donor only when NADH was present. Oxidation of 1 mol NADH gave 2 mol H_2 (Reaction (2) in the back direction). The reduction of ferredoxin and NAD^+ with H_2, which is the thermodynamically preferred reaction, was not studied (Reaction (2) in the forward direction) (Fig. 4).

The anaerobically purified hydrogenase from *T. maritima* was composed of the three subunits HydA (73 kDa), HydB (68 kDa) and HydC (18 kDa) in a 1:1:1 stoichiometry. The holoenzyme showed an apparent molecular mass of 500 kDa at pH 7 and one of 150 kDa at pH 10. The yellow brownish enzyme contained FMN, which was, however, only loosely bound and therefore had to be present in the buffers during the purification procedure; otherwise most of the activity was lost. Some of the lost activity could be restored upon addition of FMN. Surprisingly, FAD also showed a stimulatory effect albeit much less pronounced than FMN. Besides FMN the holoenzyme contained more than 30 Fe per heterotrimer. This value is, within experimental error, the sum of the values predicted from the sequence analysis (see below). Inductively coupled plasma mass spectrometry analysis (ICP) of the holoprotein did not indicate the presence of any other metal other than iron [48].

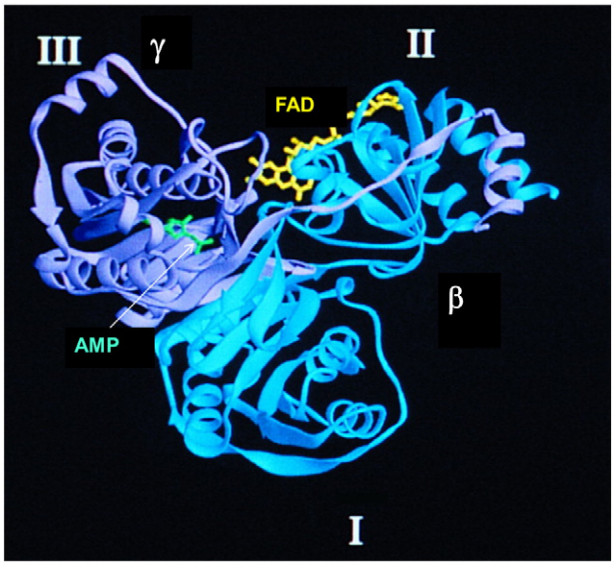

Fig. 2. Structure of the human electron transferring flavoprotein (ETF or EtfBC). The β-subunit (domains I and II) is shown in light blue and the γ-subunit (domain III) in cyan. The C-terminus of the γ-subunit wraps around domain II. PDB: 1EFV [42].

HydA is predicted by bioinformatic analyses of the encoding gene sequences to harbor the H-cluster and thus the active site interacting with H_2. This was confirmed by showing that HydA alone, after dissociation of the complex in urea, can catalyze the reduction of viologen dyes with H_2. Besides the H cluster, HydA carries 3 [4Fe–4S] and 2 [2Fe–2S] clusters. HydA shows sequence similarity (43%) to the monomeric [FeFe]hydrogenase I from *C. pasteurianum*, which catalyzes the formation of H_2 with reduced ferredoxin. HydA from *T. maritima* differs, however, in having a C-terminal extension with a [2Fe–2S] binding site which is lacking in the monomeric enzyme from *C. pasteurianum*. HydA from *T. maritima* did not catalyze the reduction of ferredoxin with H_2 nor the reverse reaction [48].

HydB shows similarity (70%) to the gene product HndC of the $NADP^+$-reducing [FeFe]hydrogenase from *Desulfovibrio fructosovorans* and to NuoF of the NADH ubiquinone oxidoreductase from *E. coli* (60% similarity). Within the sequence there are two highly conserved stretches, one characteristic for NAD^+ binding sites and the other for FMN binding sites. The C-terminal part contains Cys motifs that could bind three [4Fe–4S] clusters. At its N-terminus HydB contains four Cys residues that are thought to be involved in binding a [2Fe–2S] cluster [48]. It was not tested whether HydB alone has diaphorase activity. HydC shows four Cys residues arranged in a motif with high similarity (58%) to motifs in *E. coli* Nuo and *D. fructosovorans* HndA, which are thought to bind a [2Fe–2S] cluster.

From the experimental and bio-informatic analysis a picture of the structure and function of the HydABC complex emerges that is summarized in the cartoon shown in Fig. 4. The binding site for ferredoxin at HydC was chosen arbitrarily. Also, for the second FMN, the one with the question mark, there is no experimental evidence. The number of FMNs bound in the complex could not be determined because the FMN was lost as soon as the FMN was left out from the buffers. We postulate that two FMN should be bound, one being required

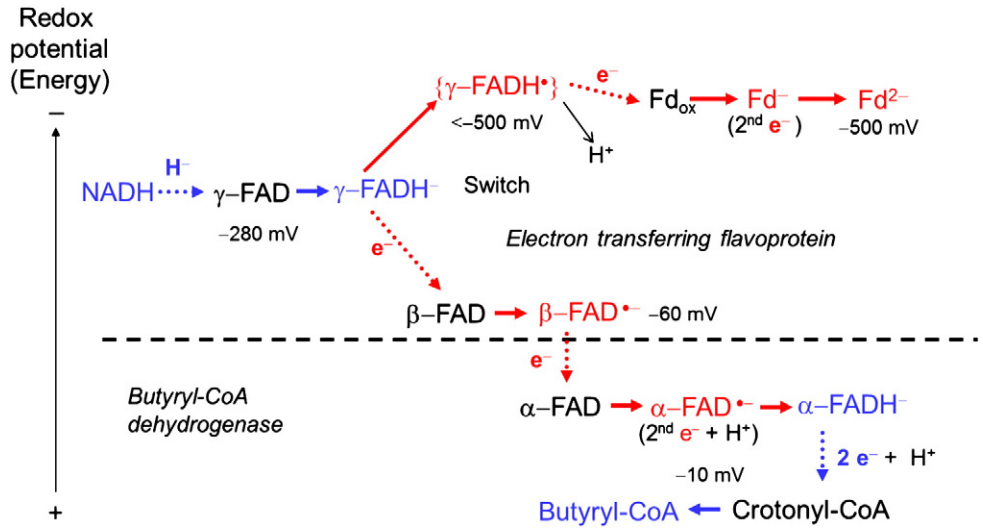

Fig. 3. Proposed mechanism of flavin based electron bifurcation for the BcdA–EtfBC. The approximate redox potentials *E'* are given in mV. Black species are oxidized, blue species are reduced by two electrons, and red species carry unpaired electrons. Dotted arrows indicate one (red) or two (blue) electron transfers. Full arrows indicate transformations. For further explanation see text.

for NADH dehydrogenation and a second one for flavin-based electron-bifurcation.

The three genes encoding HydABC in *T. maritima* are organized in a cluster *hydCBA* that is most probably a transcription unit [48]. Clustered genes for proteins with sequence similarity to HydABC are also found in many other anaerobic bacteria namely *Clostridium ljungdahlii* [49] *Acetobacterium woodii* [50] and *Moorella thermoacetica* [51]. Although these gene products have not been characterized, it was shown that cell extracts of the *A. woodii* [50] and *M. thermoacetica* [28] catalyze the NAD^+ dependent reduction of ferredoxin with H_2. Per mol ferredoxin 1 mol NAD^+ was reduced (Reaction (2) in the forward direction). In some anaerobic bacteria, e.g. *Thermoanaerobacter tengcongensis* the enzyme is composed of four rather than of three different subunits. This is due to the fact that their HydA homolog lacks the C-terminal extension with the [2Fe–2S] cluster and that these hydrogenases instead have a fourth subunit homologous to the C-terminal extension [52]. The electron-bifurcating [FeFe]hydrogenase is not found in archaea which appear to only contain [NiFe]hydrogenases and/or [Fe]hydrogenase [53].

2.3. MvhADG–HdrABC complex coupling the reduction of ferredoxin with H_2 to CoM-S-S-CoB reduction

It was long known that in cell extracts of *Methanothermobacter* species the reduction of metronidazole with H_2 is dependent on CoM-S-S-CoB, the heterodisulfide of coenzyme M (CoM-SH) and coenzyme B (CoB-SH) [54]. Metronidazole is spontaneously reduced by reduced ferredoxin and reduced flavodoxin. But it took until a year ago to show that the exergonic reduction of CoM-S-S-CoB with H_2 is coupled with the endergonic reduction of ferredoxin with H_2 (Reaction (3)). The uphill reduction of ferredoxin with H_2 driven by the exergonic reduction of CoM-S-S-CoB with H_2 could be directly demonstrated [55].

The cytoplasmic heterohexameric enzyme complex catalyzing Reaction (3) is composed of the six subunits MvhA (53 kDa), MvhG (34 kDa), MvhD (16 kDa), HdrA (72 kDa), HdrC (21 kDa) and HdrB (33 kDa) in equal amounts (Fig. 5). The complex contains about 40 Fe and acid labile sulfur/mol, one Ni, one Zn and probably one FAD which is only loosely bound and which therefore has to be added to the buffers during the purification procedure. Purification has to be performed under strictly anoxic conditions; otherwise the activity is rapidly lost (Fig. 5) [29].

The MvhADG–HdrABC complex can be dissociated into MvhADG and HdrABC. The MvhADG sub-complex catalyzes the reduction of methyl viologen with H_2 and the HdrABC sub-complex the reduction of CoM-S-S-CoB with reduced methyl viologen. MvhA harbors the [NiFe] center, which is the site of H_2 oxidation, as revealed by sequence analysis. MvhA is synthesized as a pre-protein, but the endopeptidase required for maturation has not yet been found. MvhG is the small subunit of the hydrogenase with a proximal and distal [4Fe–4S] cluster and a medial [3Fe–4S] cluster. MvhD is a [2Fe–2S] iron sulfur protein, which is of interest since in archaeal proteins [2Fe–2S] clusters are an exception. MvhD probably functions as an electronic link between the sub-complexes. In some methanogens the *mvhD* gene is associated with the *hdrABC* genes rather than with the *mvhAG* genes. In *Methanosarcina barkeri* and in *Archaeoglobus fulgidus* the *mvhD* gene is fused to the 3′-end of *hdrA* [29,53].

HdrA, which harbors the FAD binding site, carries 2 [4Fe–4S] clusters and 4 characteristically spaced cysteines which are conserved in

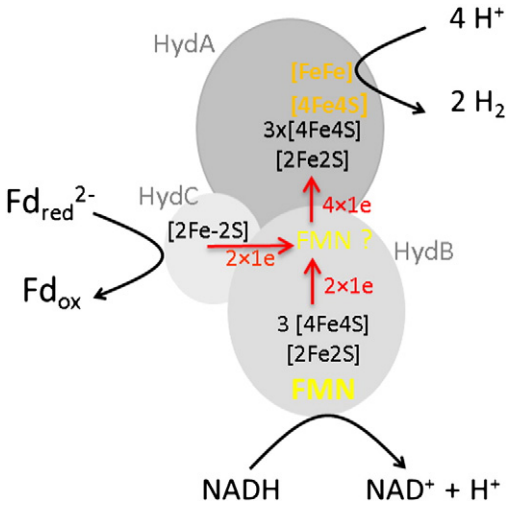

Fig. 4. Schematic representation of the structure and function the HydABC complex from *Thermotoga maritima*. The enzyme is proposed to harbor a second flavin (the one with the question mark). There is no evidence for the proposed pathway of electrons. The [FeFe] center plus [4Fe–4S] cluster colored in orange represent the H-cluster, the active site of the hydrogenase. The site of ferredoxin interaction was chosen arbitrarily.

all HdrA homologs. In HdrA from *Methanococcus* species, one of the four cysteines is replaced by a selenocysteine. HdrA is not the site of heterodisulfide reduction as previously thought. This site has been found in the zinc protein HdrB, which contains two cysteine-rich sequence motifs $C_{x31-39}CCx_{35-36}CxxC$ designated as CCG domains. The C-terminal CCG domain is involved in binding an unusual [4Fe–4S] cluster, and the N-terminal domain is involved in zinc binding. HdrC is a subunit with two [4Fe–4S] clusters. The binding site for ferredoxin at the HdrA subunit was chosen arbitrarily [55,56].

In the *Methanobacteriales*, *Methanopyrales* and *Methanococcales* the genes encoding the MvhADG–HdrABC complex are organized in three transcription units, *mvhDGAB*, *hdrA* and *hdrBC* which are not located adjacent to another. In the *Methanomicrobiales* the *hdr* genes are juxta-positioned; *mvhB* encodes for a polyferredoxin with twelve [4Fe–4S] clusters which partially purifies together with the MchADG–HdrABC complex. The gene *hdrA*, which is highly conserved, is not only found in methanogenic archaea but also in sulfate reducing archaea and some bacteria which do not contain the genes *mvhAG* and *hdrBC*. This suggests that HdrA in non-methanogens may have an electron bifurcating function within another context than in methanogens. Interesting in this respect is that in most methanogens the *hdrA* geneis located separately from the *hdrBC* genes consistent with HdrA being used not only in combination with HdrBC [56].

Many members of the *Methanomicrobiales* lack the *mvhAG* genes. It has been proposed that in these hydrogenotrophic methanogens the F_{420} reducing hydrogenase FrhAG rather than MvhAG forms a functional electron bifurcating complex [29].

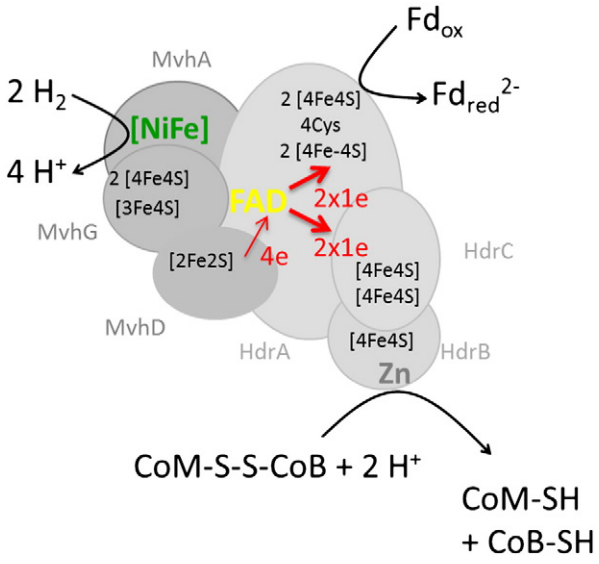

Fig. 5. Schematic representation of the structure and function of the MvhADG–HdrABC complex from *Methanothermobacter marburgensis*. The complex is found in most methanogenic archaea, exceptions being several members of the *Methanomicrobiales*. The binding site for ferredoxin (Fd) at HdrA was chosen arbitrarily. There is no evidence for the proposed pathway of electrons. The [NiFe] center of the hydrogenase is highlighted in green. Mvh, methyl viologen reducing hydrogenase; Hdr, heterodisulfide reductase.

2.4. The NfnAB complex coupling the reduction of ferredoxin with NADPH to the reduction of NAD$^+$

In 1971 it was reported that cell extracts from *C. kluyveri* catalyzed the reduction of ferredoxin with NADPH only in the presence of NAD$^+$ and that concomitant to ferredoxin also NAD$^+$ was reduced [57]. The results were interpreted to indicate that cell extracts contained an enzyme that catalyzes the reduction of ferredoxin with NADPH under the allosteric control of the NAD$^+$/NADH couple. The reduction of NAD$^+$ with NADPH was thought to be catalyzed by a separate transhydrogenase. Forty years later evidence was presented that these activities all belong to one enzyme, namely the NADH-dependent reduced ferredoxin: NADP oxidoreductase, abbreviated Nfn, Reaction (4) [27].

Nfn is a heterodimeric enzyme composed of the subunits NfnA (30 kDa) and NfnB (50 kDa) present in a 1:1 stoichiometry (Fig. 6). NfnA shows sequence similarities to ferredoxin-NADP$^+$ reductase from plants and has binding sites for NAD(P)$^+$, FAD and one [2Fe–2S] cluster. Most likely this subunit interacts with ferredoxin. NfnB shows sequence similarities to the β-subunit of the NADP$^+$-dependent glutamate synthase and also has binding sites for NAD(P)$^+$, FAD and two [4Fe–4S] clusters. During purification, the loosely bound FAD is lost with concomitant loss of activity. The activity could be partially restored by addition of FAD rather than FMN (Fig. 6).

The NfnAB complex dissociates relatively easily into NfnA and NfnB which after separation can therefore be tested separately. The UV–visible spectrum revealed that both subunits are iron–sulfur flavoproteins. Neither NfnA nor NfnB alone catalyzed Reaction (4), but when they were mixed in a 1:1 ratio, the resulting complex was active. NfnA catalyzed the reduction of benzyl viologen with NADPH (0.05 U/mg) and with NADH (0.01 U/mg), whereas NfnB catalyzed the reduction of benzyl viologen with NADPH (2 U/mg) and with NADH (0.07 U/mg). These activities did not change in the presence of NAD$^+$ or NADP$^+$. Unfortunately, from these results it cannot be deduced which subunit carries the NAD$^+$ and which the NADP$^+$ binding site.

The genes *nfnA* and *nfnB* in *C. kluyveri* are juxta-positioned and form a transcription unit. They can be heterologously expressed in *E. coli* carrying extra genes for the synthesis of iron–sulfur clusters. When expressed together, the resulting heterodimeric enzyme catalyzed Reaction (4). The heterologously produced enzyme contained only 6 to 7 irons per heterodimer. The iron content increased up to 10 after iron–sulfur cluster reconstitution. Concomitantly, the specific activity almost doubled. This finding is consistent with the presence of one [2Fe–2S] cluster and two [4Fe–4S] clusters in the heterodimer.

Genome analyses revealed the *nfnAB* genes to be present in many *Clostridiaceae*, an exception being *C. acetobutylicum*. Interestingly, in *C. ljungdahlii* the *nfnA* and *nfnB* genes are fused. They are also present in many other *Firmicutes* of the order *Clostridiales*, namely *Eubacterium*, *Thermoanaerobacter*, *Carboxidothermus*, *Desulfotomaculum* and *Moorella*. NfnAB from *M. thermoacetica* has been characterized and shown to have properties very similar to NfnAB from *C. kluyveri* [28].

The NfnAB genes are also found outside the group of the *Firmicutes* e.g. in *Bacteroides*, *Thermotoga*, *Pyrococcus*, *Thermococcus* and *Methanosarcina*. The NfnAB genes from *T. maritima* have been expressed in *E. coli* and the product has been shown to catalyze the NADH dependent reduction of NADP$^+$ with reduced ferredoxin (Reaction (4), H. Huang and R. K. Thauer, unpublished).

For NfnAB a mechanism of flavin based electron bifurcation has been proposed assuming that the FAD involved in the bifurcation is bound in the flavoprotein differently tight in its oxidized, quinone (FAD), one electron reduced, semiquinone (FADH•) and two electrons reduced, hydroquinone states (FADH$^-$) [27]: E_o' of the FAD/FADH couple in solution is −205 mV (Table 1). The redox potential E' is lower when FAD in the flavoprotein is bound more tightly than FADH$^-$. The redox potential of the FADH•/FADH$^-$ couple is more negative than that of the FADH•/FAD couple when FADH• binds tighter than FADH$^-$. In the case of n = 2 the redox potential changes by about 30 mV per factor of 10 difference in binding constants and in the case of n = 1 it changes by about 60 mV per factor of 10. It has been pointed out by Nitschke and Russell, however, that this is probably not how electron bifurcations work [47]. Their arguments are, "But why should the fully reduced flavin need the second oxidation

step to form the first one? It is already in the regime of separated 1-electron transfers and will possibly reduce ferredoxin but, even much more readily, will reduce the high potential acceptor due to the much stronger driving force for electron transfer to the latter and then just remain as a flavosemiquinone".

The "thermodynamic model" proposed by Wang et al. [27] differs from the proposed kinetic model described in Fig. 3 in the sequence of reactions. Whereas in the thermodynamic model ferredoxin is reduced by $FADH^-$ like in flavodoxins, in the kinetic model ferredoxin is reduced by the highly reactive unstable FADH• radical generated by the one electron oxidation of $FADH^-$. To discriminate between the two mechanisms, Nitschke and Russell predict that equilibrium redox titration of the flavin should demonstrate an $n = 2$ Nernst transition and a concomitant absence of a stable flavosemiquinone species [47].

2.5. Other ferredoxin-dependent enzyme complexes possibly catalyzing flavin-based electron bifurcation reactions

It has been postulated that the reduction of methylene-H_4F to methyl-H_4F ($E_o' = -200$ mV) in the acetogenic bacteria is coupled with the reduction of ferredoxin via flavin-based electron bifurcation [49]. Information on the methylene-H_4F reductase is available for *A. woodii* and *M. thermoacetica*. In *A. woodii* the gene probably encoding for methylene-H_4F reductase is found in a transcription unit of three genes that – on the protein level – show sequence similarities to the methylene-H_4F reductase from *E. coli*, to zinc finger proteins and to a NAD^+ binding flavoprotein, respectively [50]. In cell extracts methylene-H_4F is reduced specifically by NADH, the presence of ferredoxin not being required [58]. In *M. thermoacetica* the gene with sequence similarity to methylene-H_4F reductase from *E. coli* is located in a gene cluster together with genes for a zinc finger protein and four proteins homologous to Mvhd, HdrA, HdrB and HdrC that are found in the electron bifurcating MvHADG–HdrABC complex catalyzing Reaction (3) [28]. Cell extracts of *M. thermoacetica* catalyze the reduction of methylene-H_4F only with reduced viologen dyes rather than with reduced ferredoxin, NADH or NADPH, neither when tested alone or in combinations.

Another candidate for flavin-based electron bifurcation is the ATP-independent benzoyl-CoA reductase from strictly anaerobic bacteria of the genera *Geobacter* and *Syntrophus* that are energy limited [59,60]. Benzoyl-CoA is the key intermediate in the anaerobic degradation of aromatic compounds. The tungsten iron–sulfur flavoprotein from *G. metallireducens* catalyzes the reduction of benzoyl-CoA to cyclohexa-1,5-dienoyl-1-carboxyl-CoA (dienoyl-CoA) most likely with reduced ferredoxin as electron donor although this has not yet been ascertained. Thermodynamically this is an uphill reaction since the redox potential $E^{o'}$ of the dienoyl-CoA/benzoyl-CoA couple is −622 mV [59]. The uphill reduction of benzoyl-CoA to dienoyl-CoA with reduced ferredoxin must therefore somehow be coupled with a downhill oxidation of reduced ferredoxin most probably with NAD^+. The finding that the enzyme complex is composed of 8 different subunits, four of which show sequence similarities to the subunits Mvhd, HdrA, HdrB and HdrC of the electron bifurcating MvhADG–HdrABC complex from methanogenic archaea (Section 2.2), supports this proposal. Anaerobes that are not energy limited as the denitrifier *Thauera aromatica* use an ATP-dependent benzoyl-CoA reductase [22] which is not phylogenetically related to the ATP-independent enzymes.

More than 40 years ago it was found that cell extracts of *Clostridium acidi-urici* catalyze the reduction of CO_2 to formate only in the presence of reduced ferredoxin and NADH [61]. It is thus possible that the organism contains an enzyme that couples the exergonic reduction of NAD^+ by formate with the reduction of ferredoxin by formate, similar to the HydABC complex from *T. maritima* in which the hydrogenase couples the exergonic reduction of NAD^+ by H_2 with the reduction of ferredoxin by H_2 [26].

Comparative genome analysis of energy metabolism in sulfate reducing bacteria and archaea has revealed several transcription units for cytoplasmic enzyme complexes containing homologs of HdrA, HdrB and HdrC. It has been speculated that these complexes catalyze electron bifurcating reactions, especially with adenosine phosphosulfate as high potential electron acceptor ($E^{o'}$ ca. −100 mV) [62,63].

2.6. Comparison of flavin-based electron bifurcation with ubiquinone-based electron bifurcation

Electron bifurcation was first proposed by Peter Mitchell in 1976 to explain the *reduction* of the low potential cytochrome b_L in mitochondria by addition of the strong *oxidant* ferricyanide [64]. This ingenious idea resulted in the establishment of the Q-cycle, in which the oxidation of ubiquinol (QH_2) by cytochrome *c* causes the translocation of two protons per electron across the inner mitochondrial membrane [65]. An essential feature of the cycle is the two binding sites for QH_2, the Q_o and Q_i sites and that QH_2 at the Q_o-site is oxidized simultaneously by the Rieske [2Fe–2S] cluster in the iron sulfur protein (ISP) and by cytochrome b_L (cyt b_L), each of which removes one electron and the two protons are released to the outside (Fig. 7). This process has been called bifurcation, because the two electrons from QH_2 are separated to different energy levels like the tines of a fork (Latin furca = fork). One electron goes to the iron sulfur protein with a higher redox potential ($E^{o'} = +320$ mV) and the other to cyt b_L with a lower redox potential ($E^{o'} = -90$ mV) than QH_2 ($E^{o'} = +90$ mV). In the proton motive Q cycle, the one-electron oxidation of QH_2 by the Rieske cluster triggers the reduction of cyt b_L. Then the Rieske cluster in the iron sulfur protein flips over to enable the transfer of the electron to cyt c_1 ($E^{o'} = +263$ mV) and further to the final acceptor cyt *c* ($E^{o'} = +230$ mV) [66]. The electron in cyt b_L moves via cyt b_H ($E^{o'} = +50$ mV) to the Q_i-site where it reduces the bound Q to a stabilized semiquinone. The bifurcation is repeated with a second QH_2 at the Q_o-site yielding another reduced cyt *c* and a fully reduced QH_2 at the Q_i-site, whereby two protons are released again to the cytoplasm and two are taken up from the matrix. In summary one QH_2 is oxidized to afford two reduced cyt *c*, whereby four protons are translocated to the cytoplasm and two are taken up from the matrix. The other two protons stem also from the matrix during reduction of Q to QH_2 by $NADH + H^+$, succinate or two reduced one-electron transferring flavoproteins ($ETF^{\bullet -}$) [67–69].

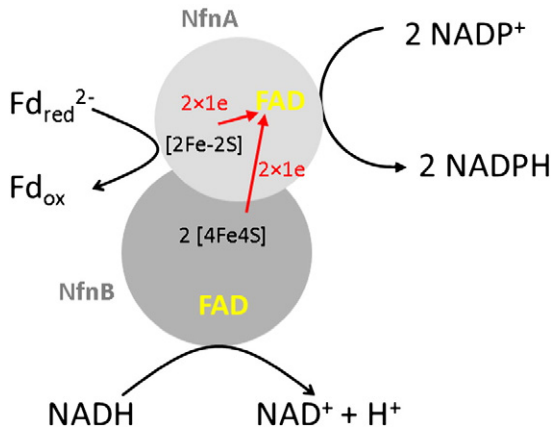

Fig. 6. Schematic representation of structure and function of the NfnAB complex from *Clostridium kluyveri*. The complex is found in most clostridia but its presence is not restricted to this genus. The binding site for ferredoxin and $NADP^+$ is assumed to be on NfnA because this subunit shows sequence similarity to ferredoxin: $NADP^+$ reductase from plants.

3. Membrane-associated enzyme complexes coupling exergonic ferredoxin oxidation reactions with vectorial proton/Na^+ translocation

The generation of reduced ferredoxin in the electron bifurcating Reactions (1)–(4) conserves part of the free energy change associated with these reactions in a redox potential ($E' = -500$ mV) which is more negative than that of the NAD^+/NADH couple ($E' = -280$ mV) and that of the H^+/H_2 couple (dependent on pH_2 between −300 mV and −414 mV) (see Introduction). The redox potential difference between ferredoxin and NAD^+ ($\Delta E' = 220$ mV) is sufficient to allow the build-up of an electrochemical proton or sodium ion potential ($\Delta\mu H^+/Na^+$) that in turn could be used to drive the phosphorylation of ADP via a membrane associated F_oF_1- or A_oA_1ATP synthase complex. The same is true for the redox potential difference between ferredoxin and protons if pH_2 is kept low by H_2-consuming microorganisms, which is the case in most anaerobic habitats. And indeed, genome sequencing revealed that many anaerobes contain the genes for a membrane associated RnfA–G complex [71] and/or a membrane associated, energy converting [NiFe]hydrogenase complex [72] catalyzing the reversible oxidation of reduced ferredoxin with NAD^+ (Reaction (6)) and H^+ (Reaction (10)), respectively.

$$Fd_{red}^{2-} + H^+ + NAD^+ \rightleftharpoons Fd_{ox} + NADH + \Delta\mu H^+/Na^+ \quad (6)$$

$$Fd_{red}^{2-} + 2H^+ \rightleftharpoons Fd_{ox} + H_2 + \Delta\mu H^+/Na^+. \quad (10)$$

3.1. RnfA–G complex coupling ferredoxin oxidation by NAD^+ with proton/Na^+ translocation

The phototrophic bacterium *Rhodobacter capsulatus* contains a cluster of six genes designated as *rnfABCDEG* that is thought to be involved in electron transfer to nitrogenase (R*hodocbacter n*itrogen *f*ixation = Rnf) [73,74]. Homologous clusters, which code for such a membrane bound NAD^+-ferredoxin oxidoreductase, are found in over a hundred aerobic and anaerobic bacteria but only in two archaea [71]. Membrane vesicles of *C. tetanomorphum* catalyze the oxidation of NADH by hexacyanoferrate(III) (ferricyanide) at a rate of 26 $U mg^{-1}$ protein and the reduction of NAD^+ by ferredoxin [reduced with Ti(III) citrate] with 1.5 $U mg^{-1}$ protein. The enzyme has been solubilized from the membrane fraction and purified to apparent homogeneity with specific activities of 400–1000 $U mg^{-1}$ protein (ferricyanide assay). The protein consists of the predicted six different subunits RnfABCDEG, which are separated by SDS-PAGE: C 49 kDa (47 kDa predicted from the gene), B 36 (30) kDa, D 33 (33) kDa, G 26 (20) kDa, A 23 (21) kDa, and E 22 (21) kDa. Sequence analysis of RnfC shows no interaction of the protein with the membrane but indicates the presence of two ferredoxin-like [4Fe–4S] clusters as well as FMN and NADH binding sites. In contrast, the sequences of RnfA, D and E reveal 6, 7 and 5 transmembrane α-helices, respectively, whereas RnfB and G appear to be anchored in the membrane by one α-helix each. RnfD and G contain covalently bound riboflavin-5′-phosphate (FMN), which is linked to the protein via a phosphodiester bond. There is also non-covalently bound FMN and riboflavin present in the enzyme complex. The determined 25 ± 1 iron atoms/hexamer match with the predicted six ferredoxin-like [4Fe–4S] clusters, two in subunit C, and four in subunit B, also called polyferredoxin [38,75–77] (Fig. 8).

Interestingly, four of the six RNF-subunits are related to four of the six subunits of the Na^+-translocating NADH-quinone oxidoreductase (Na^+-NQR) from *Vibrio cholerae* and other *Vibrio* species (Fig. 8); for a review see [78]. RnfC shares sequence identities with NqrF, RnfD with NqrB, RnfG with NqrC and RnfE with NqrD. Furthermore, NqrB (RnfD) and NqrC (RnfG) also contain covalently bound FMN. Non-covalently bound FAD + [2Fe–2S] cluster, ubiquinone-8 (Q) and riboflavin (RF) are present in subunits F, A and B, respectively [79–81]. The electrons are proposed to flow from NADH via subunits F, C, B and A to the external ubiquinone, which induce conformational changes in B triggering E and D to translocate Na^+.

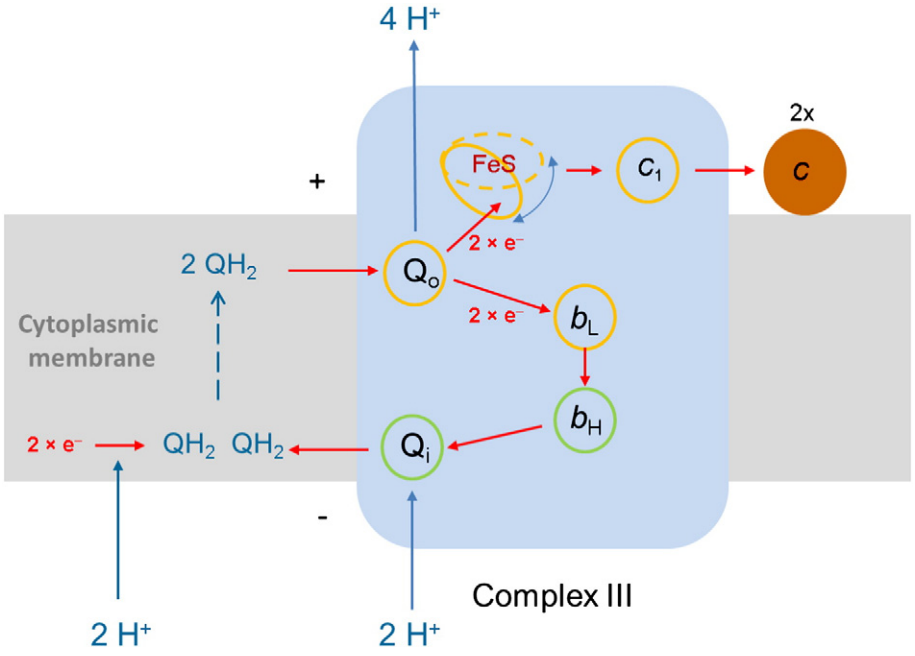

Fig. 7. Schematic presentation of the Q-cycle in complex III or cytochrome bc_1 of the mitochondrial respiratory chain. Q_i and Q_o, ubiquinone at the *i*nner and *o*uter sides of the inner mitochondrial membrane; b_l and b_H, cytochrome *b* with *l*ower and *h*igher redox potentials; FeS, Rieske [2Fe–2Fe] cluster in the iron sulfur protein; *c* and c_1, cytochrome *c* and c_1. Adapted from [70].

A similar path of the electrons, but in the opposite direction, could be constructed in Rnf: ferredoxin → RnfB → RnfD (NqrB) → RnfG (NqrC) → RnfC (NqrF) → NADH, which induces a conformational change in RnfD triggering RnfE (NqrD) and RnfA to generate an electrochemical Na^+-gradient ($\Delta\mu Na^+$, Fig. 8). It should be noted that NqrA and NqrD are not related to RnfB and Rnf A, which is certainly due to the different electron donor in Rnf (ferredoxin). Most likely, the electron flow in Rnf is reversible as proposed for nitrogen fixation in *R. capsulatus* to enable a NADH-dependent reduction of ferredoxin driven by $\Delta\mu H^+/Na^+$ [73].

Recently, it has been demonstrated that Rnf-containing membrane vesicles from *A. woodii* indeed couple the reduction of NAD^+ by reduced ferredoxin with the formation of $\Delta\mu Na^+$ that can be used for ATP-synthesis or transport processes [82] as proposed earlier for *Clostridium tetani* [83]. Similar experiments have been performed with vesicles from *C. tetanomorphum* (E. Jayamani, J. Steuber, E. Biegel, V. Müller and W. Buckel, unpublished). Notably, however, in both systems the Na^+ transport exhibited an apparent $K_m = 2.5$ mM Na^+, whereas NAD^+ reduction by ferredoxin was not stimulated by Na^+ in the range of 0.1–100 mM. In contrast, the scalar rates of established Na^+-pumps, e.g. Na^+-NQR [84], glutaconyl-CoA decarboxylase [85,86] and diphosphatase [87], are dependent on Na^+, each with K_m values for Na^+ in the lower mM range. Furthermore, with Rnf the measured Na^+ transport rates are more than 1000-times slower [82] than the scalar rate of the reduction of NADH by ferredoxin catalyzed by membrane vesicles from *C. tetanomorphum* (see above). Hence, the question whether Rnf is a real Na^+-pump or a H^+-pump that just fortuitously translocates Na^+ remains to be established.

3.2. Energy converting [NiFe]hydrogenase complexes coupling ferredoxin oxidation with proton/Na^+ translocation

Energy converting [NiFe]hydrogenases are membrane associated and catalyze the reversible reduction of ferredoxin with H_2 driven by the proton or sodium ion motive force, Reaction (10) [72]. They are found in some H_2-forming and H_2-utilizing anaerobic bacteria and archaea. Most convincing is the energy-converting function of the [NiFe]hydrogenase in the Gram-negative *Rhodospirillum rubrum* and *Rubrivivax gelatinosus* as well as the Gram-positive *Carboxidothermus hydrogenoformans*. These anaerobic bacteria can grow chemolithoautotrophically on CO, with CO_2 and H_2 being the only catabolic end products. The energy metabolism, which only involves a cytoplasmic nickel-containing carbon monoxide dehydrogenase, a cytoplasmic polyferredoxin (electron transfer protein) and a membrane associated [NiFe]hydrogenase complex is coupled with chemiosmotic energy conservation as evidenced by growth and uncoupling experiments [88].

The membrane-associated energy-converting [NiFe]hydrogenase complex involved in CO conversion to CO_2 and H_2 is composed of six different subunits of which two are integral membrane proteins (the larger one most probably involved in cation translocation) and four are peripheral membrane proteins orientated toward the cytoplasm. Of the four peripheral proteins, one carries the [NiFe]hydrogenase active site; one harbors 1 [4Fe–4S] cluster most proximal to the [NiFe] center and one harbors 2 [4Fe–4S] clusters transporting the electrons to the ferredoxin binding site. The fourth peripheral protein is without a prosthetic group. The six subunits show sequence similarities to six of the core subunits of the NADH: ubiquinone oxidoreductase (NuoA-N) (complex I of the respiratory chain) from *E. coli*. In complex I, the subunit NuoD homologous to the [NiFe] center carrying subunit lacks the N-terminal and C-terminal CxxC motifs for [NiFe] center binding [53] (Fig. 9).

An energy converting [NiFe]hydrogenase with six subunits is also found in microorganisms not growing on CO such as *E. coli*, *M. barkeri* and *M. mazei* [88]. In *E. coli* the hydrogenase is part of the formate hydrogen lyase complex catalyzing the conversion of formate to CO_2 and H_2. In the two methanogens the six-subunit [NiFe]hydrogenase differs from those in the CO hydrogen lyase complex and the formate hydrogen lyase complex only in not forming a tight complex with its ferredoxin and functionally associated oxidoreductase. Methanogens lack complex formation because the reduced ferredoxin, generated by the energy converting hydrogenase, is used in electron transfer to more than one oxidoreductase. A two [4Fe–4S] cluster-containing ferredoxin (6 kDa) from *M. barkeri*, which is most probably the ferredoxin reduced by H_2 via the hydrogenase, has been characterized [53].

Besides the six subunit energy converting [NiFe]hydrogenases there are energy converting hydrogenases, abbreviated as Mbh, which contain, in addition to the six core subunits, up to 8 integral membrane proteins as additional subunits. The MbhA-N hydrogenase is found in some members of the *Methanomicrobiales* (*Methanospirillum hungatei* and *Methanocorpusculum labreanum*) and in *Pyrococcus furiosus*, from which the enzyme complex was purified and characterized [89,90].

In most hydrogenotrophic methanogens there is a third type of energy-converting [NiFe]hydrogenase complex, EhaA–T and EhbA–Q, with up to 20 subunits of which only four show sequence similarity to subunits of the [NiFe]hydrogenase from *R. rubrum*. These are the two conserved integral membrane proteins and the two proteins harboring the [NiFe] center and the [4Fe–4S] cluster, respectively. A core subunit with 2 [4Fe–4S] clusters appears to be lacking. Instead, there is a 6 [4Fe–4S] cluster polyferredoxin (EhaP) or a 10 [4Fe–4S] cluster polyferredoxin (EhaQ) in the EhaA–T complex as well as a non-conserved 2 [4Fe–4S] cluster ferredoxin (EhbL) and a 14 [4Fe–4S] cluster polyferredoxin in the EhbA–Q complex. Of the additional other subunits most are non-conserved integral membrane proteins [53]. The standard [NiFe]hydrogenase complexes composed of the 6 core subunits probably all translocate protons, whereas the larger [NiFe]hydrogenase complexes MbhA–N, EhaA–T and EhbA–Q most probably translocate sodium ions [53].

4. Anaerobes conserving energy via electron bifurcating ferredoxin reduction and/or proton/Na^+ translocating ferredoxin oxidation

Comparisons of many energy metabolisms of aerobic and anaerobic chemotrophic organisms have revealed that between 60 and 80 kJ is required in a living cell to synthesize ATP from ADP and inorganic phosphate [11]. The higher value is more characteristic for aerobes and the lower value for anaerobes. Under equilibrium conditions only about 50 kJ/mol ATP is required. During energy conservation, the difference is dissipated as heat (Fig. 10).

The beauty of the relatively constant amount of energy required for the synthesis of ATP is the possibility to predict the numbers of ATP synthesized, provided the free energy change associated with an energy metabolism is known. This is because competition has forced microbes to maximize their thermodynamic efficiency of ATP synthesis (ATP/ΔG) [11]. In most cases the number agrees well with the number of ATP known to be generated via substrate level phosphorylation (SLP) and electron transport phosphorylation (ETP). In the energy metabolism of some anaerobes, however, there was no agreement indicating that all sites of energy conservation in the energy metabolism were not yet known. The finding of energy conservation via electron bifurcating ferredoxin reduction and of proton/Na^+ translocating ferredoxin oxidation in many anaerobes has closed this gap as will be shown in the following examples (Fig. 10).

4.1. Glucose fermentation by Clostridium pasteurianum

C. pasteurianum ferments 1.5 glucose to 1 acetate, 1 butyrate, 2 CO_2 and 4 H_2 (Fig. 11). H_2 bubbles out of the cultures indicating that the H_2 partial pressure is near 100 kPa (1 bar) and that the redox potential of the H^+/H_2 couple is at least −400 mV. Glucose is transported into the

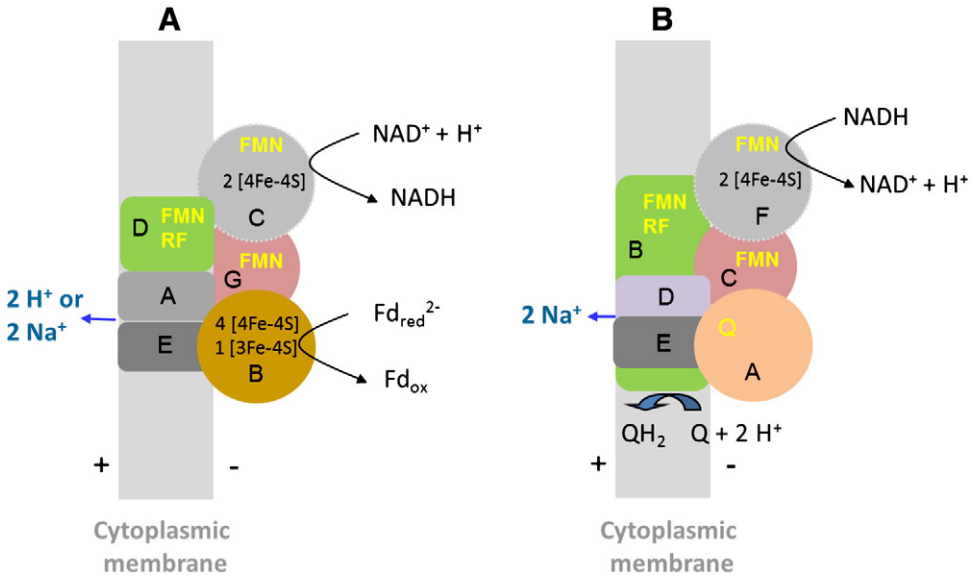

Fig. 8. A, model of H^+/Na^+-translocating NAD-ferredoxin reductase (RnfA–G) from *Clostridium tetanomorphum*. B, model of Na^+-translocating NADH-quinone oxidoreductase (Na^+-NqrA-F) from *Vibrio cholerae*, adapted from [81]; RF, riboflavin. The black letters indicate the designation of the subunits. Homologous subunits bear the same color. RnfB and G as well as NqrF and C are fixed by one transmembrane α-helix each. RnfD, A and E as well as NqrB, D and E are integral membrane proteins.

cells via a phosphoenolpyruvate (PEP) transferase system [91,92] and the oxidation to 2 pyruvate proceeds via the Embden–Meyerhof pathway, generating 3 NADH and 3 ATP per 1.5 mol glucose. The 3 pyruvates are further oxidized to 3 acetyl-CoA with 3 ferredoxin as electron acceptor. One acetyl-CoA gives rise to 1 acetate and 1 ATP and the other 2 acetyl-CoA are reduced to butyrate concomitant with the formation of 1 ATP. The organism contains a ferredoxin-dependent monomeric [FeFe]hydrogenase [93], which catalyzes the re-oxidation of the ferredoxin with the formation of H_2. Since 4 rather than 3 mol H_2 is formed per 1.5 mol glucose [11], there must be a route from NADH to ferredoxin. Considering that the redox potential of the NAD^+/NADH couple in the cells is −280 mV and that of the H^+/H_2 couple is near −400 mV, ferredoxin reduction with NADH is only possible if coupled to the exergonic crotonyl-CoA reduction with NADH. If the two reactions were not coupled, all the NADH generated in the Embden–Meyerhof pathway would have to be re-oxidized via butyric acid formation from acetyl-CoA resulting in a fermentation of 1.5 glucose to 1.5 butyrate, 3 CO_2 and 3 H_2. Thereby 4.5 mol ATP would be generated rather than 5.0 mol ATP predicted from Fig. 11 (75 kJ/ATP). Thus flavin-based electron bifurcation enhances energy conservation by 11%; in the following examples the contribution is much higher. The alternative pathway of reduced ferredoxin oxidation by NAD^+ is excluded, because the membrane fraction of *C. pasteurianum* does not contain ferredoxin: NAD^+ oxidoreductase (Rnf) activity. Consistent with that finding, the genome sequence of the closely related *Clostridium acetobutylicum* lacks genes for the RnfA–G complex [94].

4.2. Glucose fermentation by Thermotoga maritima and Pyrococcus furiosus

The extremophilic bacterium *T. maritima* thrives by fermenting 1 glucose to 2 acetate, 2 H^+, 2 CO_2 and 4 H_2 at 90 °C. At this temperature

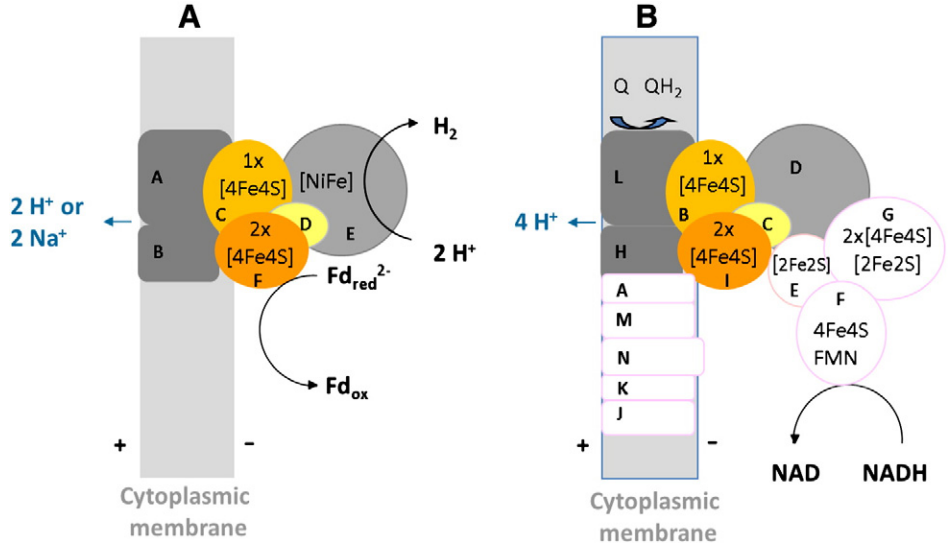

Fig. 9. Schematic representation of the structure and function of A, energy converting [NiFe]-hydrogenase EchA–F from *Rhodospirillum rubrum* and of B, energy conserving complex I from *E. coli*.

the free energy change of the reaction ($\Delta G^{o'} = -250$ kJ/mol [97]) is about 35 kJ/mol more exergonic than at 25 °C ($\Delta G^{o'} = -215$ kJ/mol) [11] allowing for the synthesis of 4 mol ATP per mol glucose from which 1 ATP has to be subtracted for glucose import mediated by a specific ABC transporter [98]. This results in an efficiency of 83 kJ/ATP even at H_2 partial pressures near 100 kPa. Glucose is fermented via the Emden–Meyerhof pathway regenerating 2 NADH and via pyruvate:ferredoxin oxidoreductase regenerating 2 reduced ferredoxin [99] (Fig. 12). The formation of 4 H_2 indicates that all reducing equivalents from NADH escape as hydrogen. To make this thermodynamically possible, the endergonic reduction of protons to H_2 with NADH is coupled to the exergonic reduction of protons to H_2 with reduced ferredoxin as catalyzed by the electron bifurcating HydABC complex [26] (Section 2.2.).

The same equation for glucose fermentation has been observed with the archaeon *P. furiosus* thriving at 100 °C, though the mechanism of energy conservation differs in many respects (Fig. 12). In this organism the phosphorylating NAD^+-dependent glyceraldehyde-3-phosphate dehydrogenase is replaced by a ferredoxin-dependent non-phosphorylating enzyme [19,100,101]. Thus only 2 ATP/glucose are obtained by SLP. However, 4 reduced ferredoxin generate 4 H_2 mediated by an energy conserving hydrogenase (Mbh) [90] (see Section 3.2.) resulting in $4 \times 2\ \Delta\mu Na^+$ equal to 2 ATP [102]. By subtracting 1 ATP for glucose import via an ABC transporter [103], the thermodynamic efficiencies of ATP synthesis in the bacterium and the archaeon are identical. The *P. furiosus* fermentation also demonstrates that reduced ferredoxin can be regarded as an 'energy rich' compound due to its more negative redox potential as compared to that of the H^+/H_2 couple. Whereas, thioesters and anhydrides are 'energy rich' because of their $\Delta G^{o'}$ of hydrolysis ≤ -30 kJ/mol ($= \Delta G^{o'}$ of ATP-hydrolysis), reduced ferredoxin with an $E' = -500$ mV is 'energy rich' because of its physiological more negative $\Delta E'$ ($\Delta G' = -n\ F\ \Delta E'$) as compared to $E' > -414$ mV of the H^+/H_2 couple and to $E' > -320$ mV of the NAD^+/NADH couple.

4.3. Ethanol–acetate fermentation of Clostridium kluyveri

C. kluyveri grows on ethanol, acetate as energy source and acetate and CO_2 as carbon source. Fermentation products are butyrate, caproate, and one proton per 2 H_2, whereby 1 ATP is formed via SLP [104]. The cells contain a ferredoxin-dependent monomeric [FeFe]hydrogenase for the generation of H_2 and a pyruvate:ferredoxin oxidoreductase for the synthesis of pyruvate from acetyl-CoA and CO_2 [34]. Until recently it was not known how the 2.5 mol ATP (72 kJ/ATP) is generated that is predicted from the free energy change associated with the fermentation ($\Delta G^{o'} = -180$ kJ/mol H^+) (Fig. 13A). It was also not known how the reduced ferredoxin required for the two reactions is regenerated. The finding that in *C. kluyveri* the exergonic reduction of crotonyl-CoA to butyryl-CoA is coupled with the endergonic reduction of ferredoxin with NADH via the BcdA–EtfBC complex (Section 2.1) and that the organism contains an RnfA–G complex (Section 3.1.) has solved these questions [25,34].

In the ethanol acetate fermentation the number of substrates exceeds the number of products. Therefore, when the concentration decreases to 1 mM, the free energy change decreases to −77 kJ/mol H^+ that can only support the synthesis of 1 ATP (Fig. 13B). (In the calculation the concentrations of water, 55.5 M, and protons, pH 7.0, do not change and therefore are not considered). The switch from 2.5 ATP to 1 ATP is realized by two additional enzymes, namely the electron bifurcating NfnAB complex and a $NADP^+$ dependent β-hydroxybutyryl-CoA dehydrogenase [34]. By tuning the activities of these two enzymes, *C. kluyveri* can maintain the efficiency of ATP synthesis constant when the free energy available in the environment changes. Whether regulation is on the transcriptional level or on the posttranslational level is not yet known [27].

4.4. Glutamate fermentation by Clostridium tetanomorphum and Acidaminococcus fermentans

Glutamate is fermented in several anaerobic bacteria of the phyla *Firmicutes* and *Fusobacteria* by two different pathways to identical products (Fig. 14): ammonia, CO_2, acetate, butyrate and hydrogen, $\Delta G^{o'} = -317$ kJ/mol H_2 [105,106]. According to the balanced fermentation equation, fewer molecules are consumed than produced (Fig. 14). Therefore, the free energy $\Delta G'$ becomes more negative at lower concentrations (see Section 4.3). Assuming the physiological concentrations of glutamate, acetate, butyrate and ammonia to be 1 mM each, $\Delta G'$ decreases to –450 kJ/mol H_2.

C. tetanomorphum and *C. tetani* ferment glutamate via 3-methylaspartate to ammonia, acetate and pyruvate mediated by the coenzyme B_{12}-dependent glutamate mutase [107] and three further enzymes (Fig. 14). Five pyruvates are then oxidized to 5 acetyl-CoA and 5 reduced ferredoxin (Fd^{2-}_{red}) that are converted together with an additional Fd^{2-}_{red} to 6 NADH mediated by Rnf yielding 12 $\Delta\mu Na^+$. Four acetyl-CoA are reduced by 6 NADH to 2 butyryl-CoA, in whose syntheses flavin-based electron bifurcation is involved resulting in additional 2 Fd^{2-}_{red}, one of which reduces protons to H_2. Three ATP are formed by SLP from 1 acetyl-CoA and 2 butyryl-CoA [23]. For the import of 5 glutamate probably 5 $\Delta\mu Na^+$ are consumed [83], leaving 7 $\Delta\mu Na^+$ for the synthesis of further 1.75 ATP, all together 0.95 ATP/glutamate with the high efficiency of 67 kJ/mol ATP under standard conditions. At lower concentrations the efficiency decreases; at the assumed 1 mM physiological concentrations (see above) it reaches 96 kJ/mol ATP.

The pathway via 2-hydroxyglutarate in *A. fermentans* (Fig. 14) transforms 5 glutamate to 5 ammonia and $5 \times (R)$-2-hydroxyglutarate that are activated by $5 \times$ acetyl-CoA to $5 \times$ 2-hydroxyglutaryl-CoA. Subsequent dehydration affords $5 \times$ glutaconyl-CoA that are decarboxylated to $5 \times$ crotonyl-CoA catalyzed by the biotin-containing membrane enzyme glutaconyl-CoA decarboxylase (Gcd) that converts the free energy of decarboxylation to an electrochemical Na^+ gradient resulting in 10 $\Delta\mu Na^+$ [85]. Three of 5 crontonyl-CoA are oxidized to 6 acetyl-CoA with the formation of 3 NADH, which together with a fourth NADH are consumed in the reduction of the remaining 2 crotonyl-CoA to 2 butyryl-CoA concomitant with electron bifurcation leading to 2 Fd^{2-}_{red}. One Fd^{2-}_{red} gives rise to H_2, and the other recycles the fourth NADH via Rnf adding 2 $\Delta\mu Na^+$ to the conserved energy [23]. If 5 $\Delta\mu Na^+$ for sodium-glutamate symport [108] are subtracted from 12 $\Delta\mu Na^+$, the net yield of ATP is identical to that via 3-methylaspartate.

As indicated above the thermodynamic efficiency of ATP synthesis is only about 100 kJ/ATP when the two organisms ferment glutamate at 1 mM substrate and product concentrations using the pathways shown in Fig. 14. This very low efficiency is not very likely. It can therefore be predicted that the two organisms increase their efficiency by changing the pathways such that the H_2 production is increased

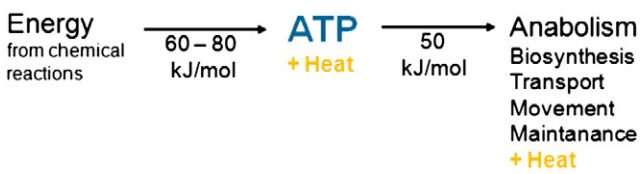

Fig. 10. ATP as central energy carrier in all living cells. Under standard reversible conditions 32 kJ/mol is required for the synthesis of 1 mol ATP from ADP and inorganic phosphate. Under physiological conditions (concentrations of ATP, ADP and P_i = 1 mM rather than 1 M) the value is −50 kJ/mol. Under the irreversible conditions in living cells, it generally takes between 60 and 80 kJ to drive the phosphorylation of ADP.

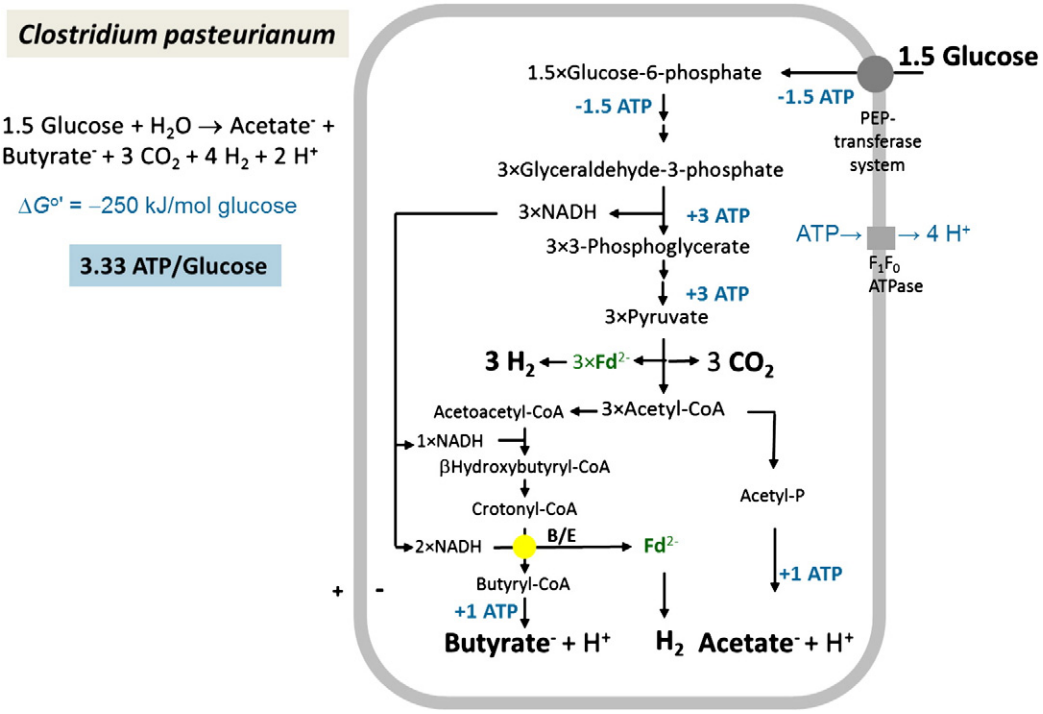

Fig. 11. Glucose fermentation by *Clostridium pasteurianum*. The F_1F_o ATPase functions in the direction of ATP hydrolysis rather than ATP synthesis [95,96]. PEP, phosphoenolpyruvate; Fd, ferredoxin; B/E, BcdA–EtfBC complex (yellow spot).

when the concentrations of substrate and products are low as they are in the natural environments where these organisms thrive. That such a change indeed may occur has been demonstrated for *C. kluyveri* in the previous chapter (Section 4.3).

Via the methylaspartate pathway [85,86] the fermentation of glutamate could proceed to acetate and H_2 without butyrate production [109]: Glutamate$^-$ + 2 $H_2O \rightarrow NH_4^+ + CO_2 + 2$ Acetate$^-$ + H_2; $\Delta G^{\circ\prime} = -45$ kJ/mol glutamate; $\Delta G'$ (1 mM) = −113 kJ/mol glutamate.

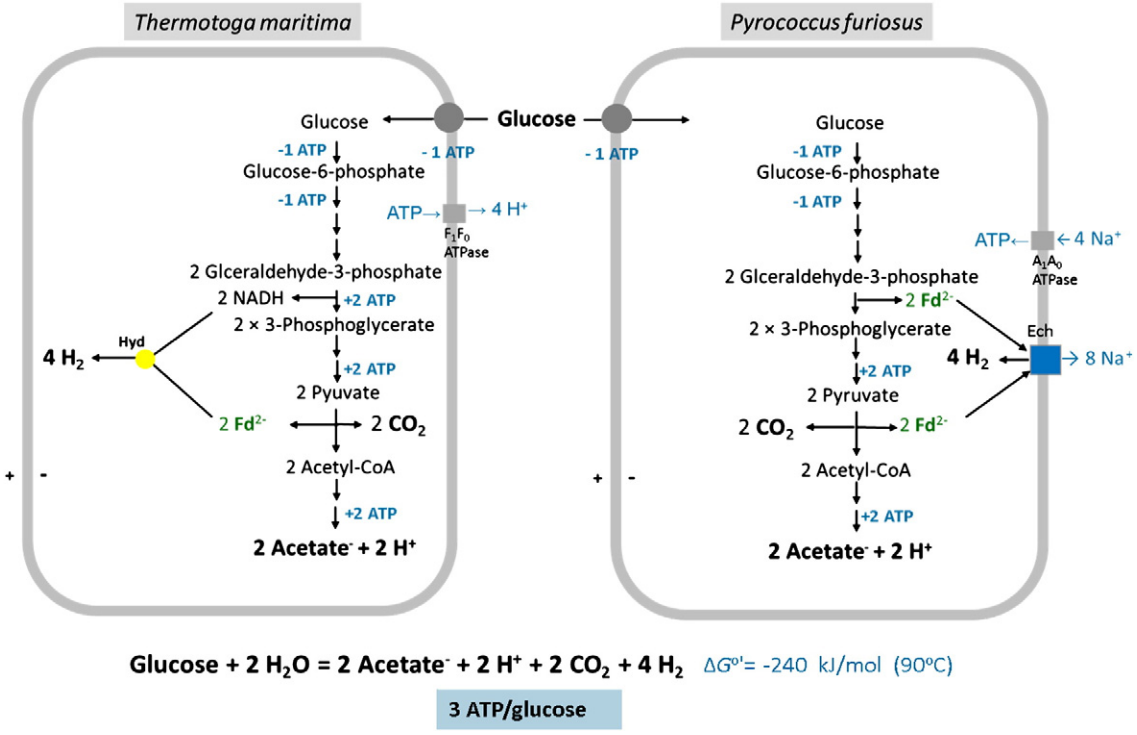

Fig. 12. Glucose fermentation in the hyperthermophilic bacterium *Thermotoga maritima* and the hyperthermophilic archaeon *Pyrococcus furiosus*. In *T. maritima* the A_1A_o ATPase functions in the direction of ATP hydrolysis rather than ATP synthesis. Fd^{2-}, reduced ferredoxin; Hyd, bifurcating hydrogenase (yellow spot); Ech, energy converting [NiFe] hydrogenase.

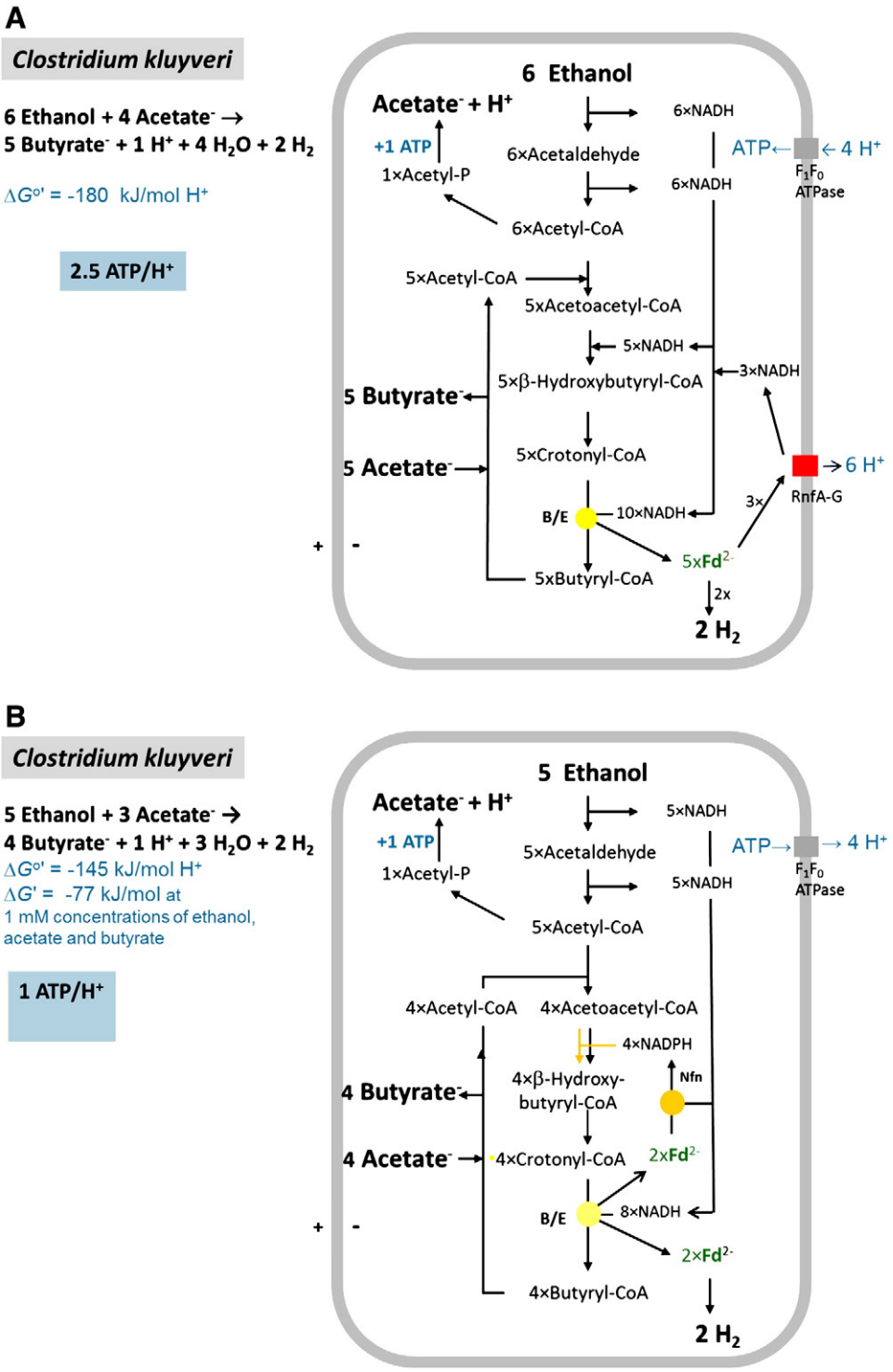

Fig. 13. Ethanol–acetate fermentation of *C. kluyveri*. A, at high ethanol and acetate concentrations; B, at low ethanol and acetate concentrations. At low substrate concentrations RnfA–G is not operative and the F_1F_o ATPase functions in the direction of ATP hydrolysis rather than ATP synthesis. The organism contains a NAD^+ specific (black arrow) and a $NADP^+$ specific (orange arrow) β-hydroxybutyryl-CoA dehydrogenase whose activities are regulated. Fd, ferredoxin; B/E, BcdA–EtfBC complex (yellow spot); Nfn, NfnAB complex (orange spot).

The formation of 1 ATP/glutamate would be possible via SLP without using bifurcation and Rnf. A route via 2-oxoglutarate and succinyl-CoA could lead to methylmalonyl-CoA that decarboxylates to propionyl-CoA [110]: Glutamate$^-$ + 2 H_2O + H^+ → NH_4^+ + 2 CO_2 + Propionate$^-$ + H_2; $\Delta G^{\circ\prime} = -19$ kJ/mol glutamate; $\Delta G'$ (1 mM) = −53 kJ/mol glutamate. Thus SLP from propionyl-CoA via propionylphosphate generating 1 ATP would be possible only in a consortium with syntrophic bacteria and methanogenic archaea. In addition 1 $\Delta\mu Na^+$ could be conserved by the sodium translocating methylmalonyl-CoA decarboxylase and used for the sodium-glutamate symporter, both of which are

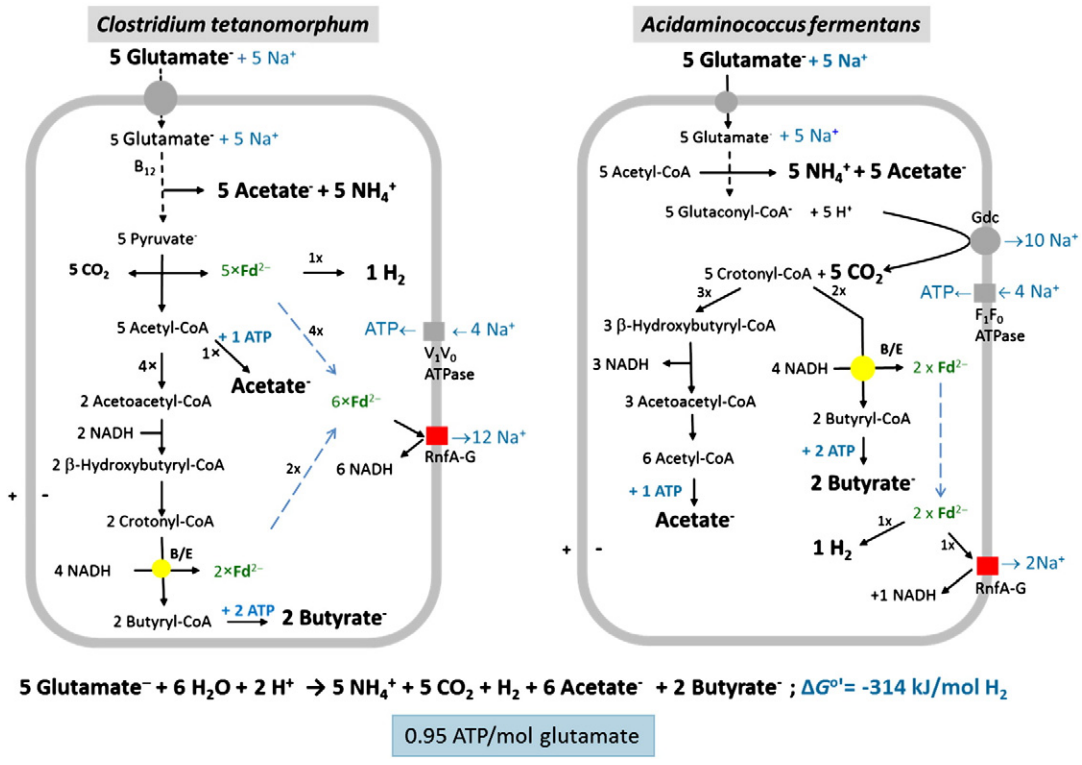

Fig. 14. Fermentation of glutamate to acetate and butyrate by two different pathways. B/E = bifurcating Bcd–Etf; Gcd = Na^+-translocating glutaconyl-CoA decarboxylase. The glutamate Na^+-symporters as well as the F_1F_o and V_1V_o ATPases are deduced from the genomes of *A. fermentans* and *C. tetani*, a relative of *C. tetanomorphum*.

present in *A. fermentans* [108,111]. However, the also required coenzyme B_{12}-dependent methylmalonyl-CoA mutase could not be detected in the genome.

4.5. Methane formation from CO_2 and H_2 by methanogenic archaea

Methanogens growing on H_2 and CO_2 generally do this in environments where the H_2 partial pressure is very low, near 10 Pa. Under these conditions the free energy change associated with CO_2 reduction to methane is about −40 kJ/mol, which is only sufficient to drive the phosphorylation of 0.5 ADP. Substrate level phosphorylation is not involved (Fig. 15) [29].

In the energy metabolism there are two coupling sites: (i) the exergonic transfer of the methyl-group of methyl-tetrahydromethanopterin to coenzyme M ($\Delta G^{o'} = -30$ kJ/mol) catalyzed by the membrane associated MtrA–H complex and coupled with the build-up of an electrochemical sodium ion potential [112], and (ii) the coupled reduction of ferredoxin and of the CoM-S-S-CoB heterodisulfide with 2 H_2 via electron bifurcation catalyzed by the MvhADG–HdrABC complex [55] (Fig. 5). The reduced ferredoxin is required for the reduction of CO_2 to formyl-methanofuran, which is the first step in methanogenesis from CO_2. The redox potential $E^{o'}$ of the CO_2/formyl-methanofuran couple is −500 mV. An energy converting hydrogenase (Section 3.2) replenishes the reduced ferredoxin required for the anabolic reduction of CO_2 to pyruvate which involves a ferredoxin-dependent reduction of CO_2 to CO ($E^{o'} = -520$ mV) and a ferredoxin-dependent reduction of acetyl-CoA + CO_2 to pyruvate ($E^{o'} = -500$ mV) [29,53].

The methanogens growing on H_2 and CO_2 using the pathway as outlined in Fig. 15 do not contain cytochromes. Methanogens with cytochromes cannot grow on H_2 and CO_2 at H_2 partial pressures as low as 10 Pa [29,55]. They couple chemiosmotically the exergonic reduction of CoM-S-S-CoB with H_2 and the endergonic reduction of ferredoxin with H_2 [113].

4.6. Acetic acid formation from CO_2 and H_2 by acetogenic bacteria

The threshold concentration of acetogens for H_2 (200 Pa) is much higher than that of methanogens (10 Pa) [50]. At 200 Pa the free energy change associated with acetogenesis from H_2 and CO_2 is only about −35 kJ which is sufficient for the synthesis of about 0.5 mol ATP. How these 0.5 mol ATP are generated is still not known, neither in *A. woodii* (contains no cytochromes) nor in *M. thermoacetica* (contains cytochromes), which are the best studied model organisms (Fig. 16). In both organisms the ATP generated in the acetate kinase reaction via SLP is required for the activation of formate to formyl-tetrahydrofolate (formyl-H_4F). Thus no net ATP is formed via SLP.

It has recently been proposed, how in *A. woodii* energy is conserved [50]. *A. woodii* contains an electron bifurcating [FeFe]hydrogenase catalyzing the coupled reduction of NAD^+ and ferredoxin with 2 H_2, similar to the HydABC complex in Section 2.2. Two of the enzymes involved in CO_2 reduction to acetic acid are NAD^+-specific (methylene-H_4F dehydrogenase and methylene-H_4F reductase), one is ferredoxin specific (CO dehydrogenase) and one (formate dehydrogenase) is in a complex with a second [FeFe]hydrogenase. The organism contains an energy conserving RnfA–G complex [82] rather than an energy converting [NiFe]hydrogenase complex [50]. With this information the metabolic scheme shown in Fig. 16 can be drawn predicting that per mol acetic acid formed from H_2 and CO_2 only 0.25 mol ATP is generated. The scheme does not include the proposal that the methylene-H_4F reductase could be electron bifurcating [50] because it could not yet be demonstrated that the methylene-H_4F reductase couples the exergonic reduction of methylene-H_4F ($E^{o'} = -200$ mV) by NADH with the reduction of ferredoxin.

M. thermoacetica also contains the electron bifurcating [FeFe]hydrogenase HydABC catalyzing the coupled reduction of NAD^+ and ferredoxin with 2 H_2 and, in addition, an electron bifurcating transhydrogenase catalyzing the coupled reduction of two $NADP^+$

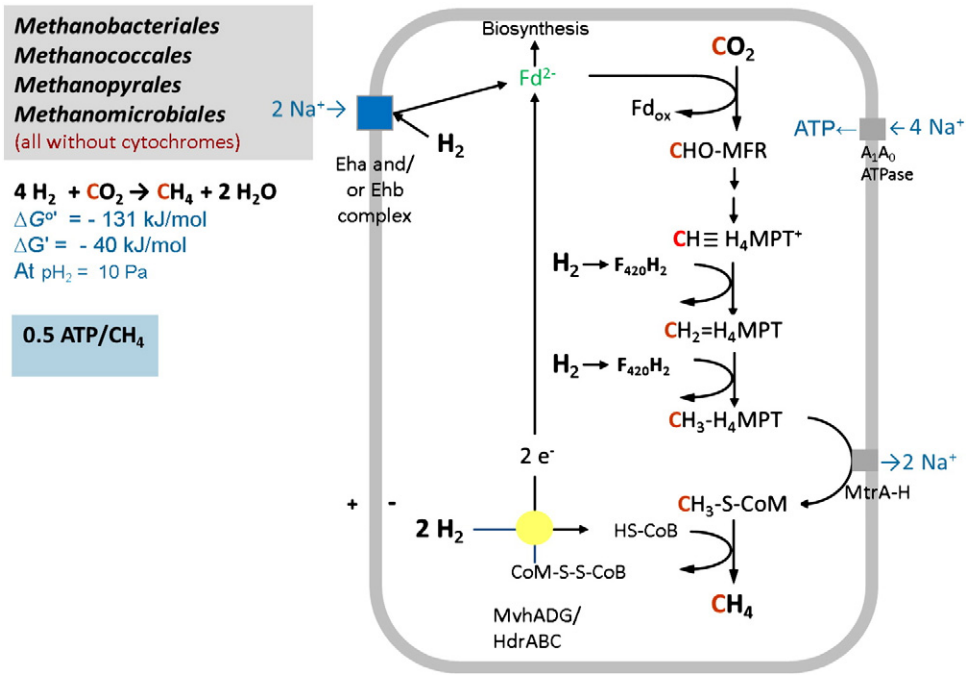

Fig. 15. Methane formation from H_2 and CO_2 by methanogenic archaea without cytochromes. CHO-MFR, formyl-methanofuran; CH≡H_4MPT, methenyl-tetrahydromethanopterin; CH_2=H_4MPT, methylene-tetrahydromethanopterin; CH_3-H_4MPT, methyl-tetrahydromethanopterin; CH_3-S-CoM, methyl-coenzyme M; CoM-S-S-CoB, heterodisulfide of coenzyme M and coenzyme B; Fd, ferredoxin; Eha and Ehb, energy converting hydrogenases; Mtr, methyltransferase. Mvh, methyl viologen reducing hydrogenase; Hdr, heterodisulfide reductase.

with reduced ferredoxin and NADH [28] (Fig. 16). Two of the enzymes involved in CO_2 reduction to acetic acid are $NADP^+$ specific (formate dehydrogenase and methylene-H_4F dehydrogenase), one enzyme is ferredoxin specific (CO dehydrogenase) and one is of unknown electron donor specificity (methylene-H_4F reductase). It has been proposed that the exergonic reduction of methylene-H_4F to methyl-H_4F ($E^{o'} = -200$ mV) with H_2 could somehow drive the reduction of ferredoxin, which in turn could be oxidized by protons via the energy converting [NiFe]–hydrogenase complex (EchA-G) present in *M. thermoacetica* which lacks genes for an energy conserving RnfA–G complex [28]. Experimental evidence for this coupling mechanism is, however, not yet available.

5. Discussion

In this review we have described that many anaerobes contain cytoplasmic flavin-containing enzymes that catalyze the reduction of ferredoxin by an electron donor with a more positive redox potential than that of ferredoxin ($E'_{donor} - E'_{ferredoxin} = \Delta E_1 > 0$). This is accomplished by coupling the oxidation of the same donor by an acceptor with a more positive redox potential than that of the donor ($E'_{acceptor} - E'_{donor} = \Delta E_2 > 0$). This process, called flavin based electron bifurcation, is only possible if $\Delta E_2 \geq \Delta E_1$, otherwise it cannot proceed. The flux of the bifurcation should be proportional to the difference $\Delta E_2 - \Delta E_1$, which is equivalent to the overall $\Delta G^{o'}$ of the bifurcation. Via the oxidation of the reduced ferredoxin thus generated, either with NAD^+ (energy conserving reduced ferredoxin: NAD^+ oxidoreductase, Rnf, mainly in bacteria) or with H^+ (energy converting [NiFe]hydrogenases in archaea and bacteria) the negative electron potential of the reduced ferredoxin is converted into an electrochemical proton or sodium ion potential which in turn drives the phosphorylation of ATP. The clostridial [FeFe]hydrogenases also contribute to energy conservation, because the reduction of protons to H_2 saves substrate as electron acceptor and thus increases substrate oxidation to 'energy rich' intermediates for SLP. We showed with 9 examples how via flavin-based electron bifurcation and/or chemiosmotic coupling the "last drop of free energy is squeezed out of the fermentations for the synthesis of as much ATP as possible" [47]. We did not mention until now that there may be exceptions from this rule.

Clostridium propionicum ferments 3 alanine to 3 ammonia, 1 acetate, 1 CO_2 and 2 propionate via the acrylyl-CoA pathway. By a related pathway *Megasphaera elsdenii* converts 6 lactate to 4 CO_2, 2 H_2, 1 acetate, 1 propionate, 1 butyrate, 1 valerate and traces of caproate. The free energy changes associated with these fermentations are −49 kJ/mol alanine and −46 kJ/mol lactate. This is sufficient to allow for the phosphorylation of at least ⅔ ADP/alanine or lactate but all available evidence indicates that only about 0.5 ATP is generated via SLP and electron transport phosphorylation without bifurcation. The purified propionyl-CoA dehydrogenase/Etf complex was reported to catalyze the reduction of acryl-CoA with NADH without the requirement of ferredoxin [114], although its amino acid sequences share high identities to those of the Bcd–Etf complex from *C. kluyveri*. Similarly, the purified Etf from *M. elsdenii* in combination with the butyryl-CoA dehydrogenase appears to mediate the reduction of crotonyl-CoA by NADH without ferredoxin [115], though this system is closely related to the bifurcating system from *A. fermentans* (see Section 2.1). Both, *M. elsdenii* and *A. fermentans*, belong to the family *Acidaminococcaceae*, the only Gram-negative family among the phylum *Firmicutes*. Finally, the growth yield of *Clostridium homopropionicum* fermenting alanine via acrylyl-CoA to propionate is about half as high as that of *Propionibacterium freundenreichii* which uses the methylmalonyl-CoA pathway for propionate production [116]. Hence, the propionyl-CoA dehydrogenases/EtfBC complexes from *C. propionicum* and *C. homopropionicum* as well as EtfBC from *M. elsdenii* might be regarded as mutants that lost the ability of bifurcation to cope with the highly reactive electrophilic and therefore toxic acrylyl-CoA [117,118]. These examples strongly indicate that organisms avoid bifurcation with acrylyl-CoA, though its redox potential of $E^{o'} = +69$ mV would favor this process even better than crotonyl-CoA ($E^{o'} = -10$ mV) [10]. Without

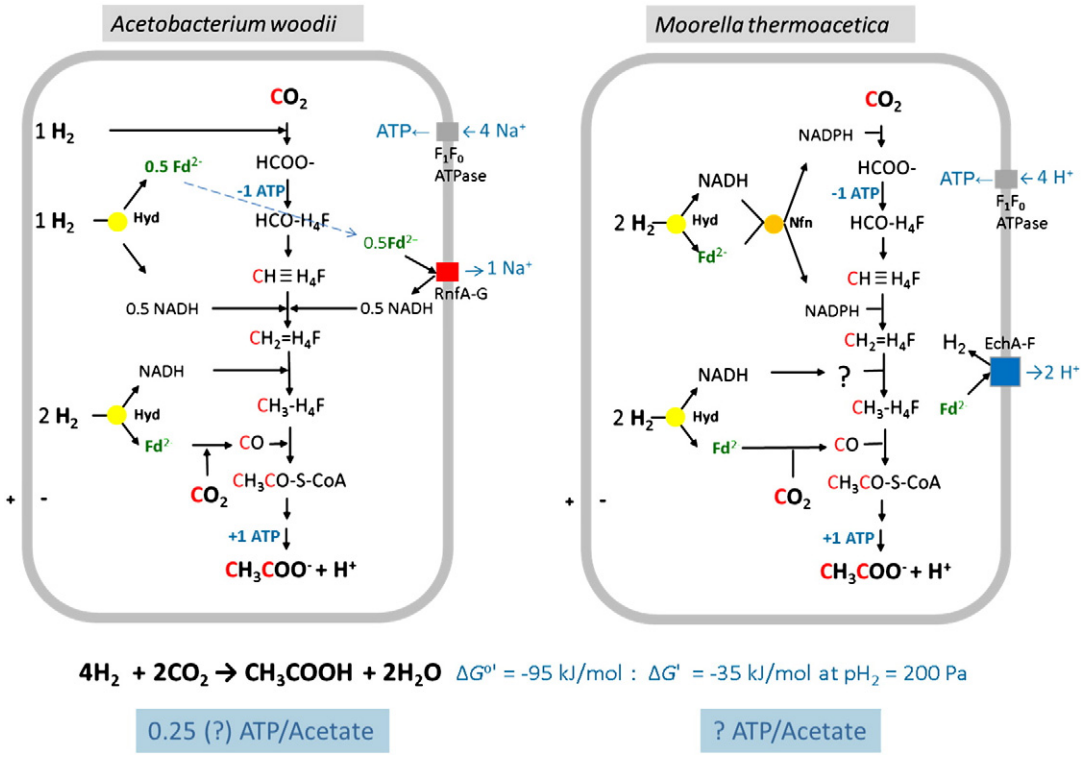

$4H_2 + 2CO_2 \rightarrow CH_3COOH + 2H_2O$ $\Delta G^{\circ\prime} = -95$ kJ/mol : $\Delta G' = -35$ kJ/mol at $pH_2 = 200$ Pa

0.25 (?) ATP/Acetate ? ATP/Acetate

Fig. 16. Acetic acid formation from H_2 and CO_2 by *Acetobacterium woodii* (does not contain cytochromes) and *Moorella thermoacetica* (contains cytochromes). HCO–H_4F, formyl-tetrahydrofolate; CH≡H_4F, methenyl-tetrahydrofolate; CH_2=H_4F, methylene-tetrahydrofolate; CH_3-H_4F, methyl-tetrahydrofolate; Fd^{2-}, reduced ferredoxin; EchA–F, energy converting hydrogenases; RnfA–G, energy conserving reduced ferredoxin: NAD oxidoreductase.

bifurcation the steady state concentration of the toxic acrylyl-CoA should be much lower. In this respect it is of interest that some facultative bacteria contain enzyme complexes with the cytochrome b_Lb_H module, which do not use quinone-based electron bifurcation [119], probably due to thermodynamic reasons (Section 2.6).

The four cytoplasmic enzyme complexes shown to catalyze electron bifurcation reactions have in common that they all contain at least one flavin, which is the reason why we assume that electron bifurcation in all four enzyme complexes is flavin based. But this does not necessarily have to be true. It has been suggested that in addition to ubiquinone and flavins other compounds such as W^{IV} and Mo^{IV} and possibly even H_2 could be electron bifurcating [47,120,121]. The formate dehydrogenase from *C. acidi-urici*, which catalyzes the ferredoxin-dependent reduction of NAD^+ with formate, is most probably a molybdenum protein (Section 2.5) [61]. Although this enzyme has not yet been purified and characterized, we envisage that this enzyme could catalyze a molybdenum-based electron bifurcation reaction. The current hypotheses of the origin of life mainly focus on a chemolithoautotrophic start with the reduction of atmospheric CO_2 to acetate by hydrogen produced by reduction of H_2O with Fe^{II} in the earth's crust. As shown in Fig. 16, acetogenesis relies on electron bifurcation, due to the inability of hydrogen, especially at pressures far below 10^5 Pa, to efficiently reduce CO_2 to CO. Hence, bifurcation might have driven the evolution of the first biochemical pathways [121].

Finally we want to add B_{12} to the list of possibly electron bifurcating compounds. B_{12} with its two-redox transitions from cob(I)alamin via cob(II)alamin to cob(III)alamin could also do the electrochemical trick of oxidation triggered reductions [47]. Anaerobic bacteria growing on H_2 with halogenated compounds as electron acceptors involve cob(I)alamin in reductive dehalogenation reactions [122–125]. How this exergonic reaction is coupled with energy conservation is not yet known. B_{12}-based electron bifurcation in dehalorespiration is therefore something to think about.

Note added in proof

In the meantime it was found that Bcd together with Etf from M. elesdenii catalyze the crotonyl-CoA-dependent reduction of ferredoxin with NADH only under strictly anaerobic conditions (N. Pal Chowdhury and W. Buckel).

Acknowledgements

This work was supported by funds from the Max-Planck-Gesellschaft and by the Fonds der Chemischen Industrie.

References

[1] W. Lovenberg, B.B. Buchanan, J.C. Rabinowitz, Studies on the chemical nature of clostridial ferredoxin, J. Biol. Chem. 238 (1963) 3899–3913.
[2] D.C. Yoch, R.C. Valentine, Four-iron (sulfide) ferredoxin from *Bacillus polymyxa*, J. Bacteriol. 110 (1972) 1211–1213.
[3] L.H. Jensen, X-ray structural studies of ferredoxin and related electron carriers, Annu. Rev. Biochem. 43 (1974) 461–507.
[4] E.T. Smith, J.M. Tomich, T. Iwamoto, J.H. Richards, Y. Mao, B.A. Feinberg, A totally synthetic histidine-2 ferredoxin: thermal stability and redox properties, Biochemistry 30 (1991) 11669–11676.
[5] W. Thamer, I. Cirpus, M. Hans, A.J. Pierik, T. Selmer, E. Bill, D. Linder, W. Buckel, A two [4Fe–4S]-cluster-containing ferredoxin as an alternative electron donor for 2-hydroxyglutaryl-CoA dehydratase from *Acidaminococcus fermentans*, Arch. Microbiol. 179 (2003) 197–204.
[6] B.D. Bennett, E.H. Kimball, M. Gao, R. Osterhout, S.J. Van Dien, J.D. Rabinowitz, Absolute metabolite concentrations and implied enzyme active site occupancy in *Escherichia coli*, Nat. Chem. Biol. 5 (2009) 593–599.
[7] R.D. Draper, L.L. Ingraham, A potentiometric study of the flavin semiquinone equilibrium, Arch. Biochem. Biophys. 125 (1968) 802–808.
[8] M. Hans, E. Bill, I. Cirpus, A.J. Pierik, M. Hetzel, D. Alber, W. Buckel, Adenosine triphosphate-induced electron transfer in 2-hydroxyglutaryl-CoA dehydratase from *Acidaminococcus fermentans*, Biochemistry 41 (2002) 5873–5882.
[9] M. Husain, M.T. Stankovich, B.G. Fox, Measurement of the oxidation–reduction potentials for one-electron and two-electron reduction of electron-transfer flavoprotein from pig liver, Biochem. J. 219 (1984) 1043–1047.

[10] K. Sato, Y. Nishina, C. Setoyama, R. Miura, K. Shiga, Unusually high standard redox potential of acrylyl-CoA/propionyl-CoA couple among enoyl-CoA/acyl-CoA couples: a reason for the distinct metabolic pathway of propionyl-CoA from longer acyl-CoAs, J. Biochem. 126 (1999) 668–675.

[11] R.K. Thauer, K. Jungermann, K. Decker, Energy conservation in chemotrophic anaerobic bacteria, Bacteriol. Rev. 41 (1977) 100–180.

[12] P.A. Bertram, R.K. Thauer, Thermodynamics of the formylmethanofuran dehydrogenase reaction in *Methanobacterium thermoautotrophicum*, Eur. J. Biochem. 226 (1994) 811–818.

[13] M. Tietze, A. Beuchle, I. Lamla, N. Orth, M. Dehler, G. Greiner, U. Beifuss, Redox potentials of methanophenazine and CoB-S-S-CoM, factors involved in electron transport in methanogenic archaea, Chembiochem 4 (2003) 333–335.

[14] J.S. Chen, L.E. Mortenson, Purification and properties of hydrogenase from *Clostridium pasteurianum* W5, Biochim. Biophys. Acta 371 (1974) 283–298.

[15] K. Uyeda, J.C. Rabinowitz, Pyruvate–ferredoxin oxidoreductase. 3. Purification and properties of the enzyme, J. Biol. Chem. 246 (1971) 3111–3119.

[16] K.C. Terlesky, J.G. Ferry, Ferredoxin requirement for electron transport from the carbon monoxide dehydrogenase complex to a membrane-bound hydrogenase in acetate-grown *Methanosarcina thermophila*, J. Biol. Chem. 263 (1988) 4075–4079.

[17] J. Heider, K. Ma, M.W. Adams, Purification, characterization, and metabolic function of tungsten-containing aldehyde ferredoxin oxidoreductase from the hyperthermophilic and proteolytic archaeon *Thermococcus* strain ES-1, J. Bacteriol. 177 (1995) 4757–4764.

[18] P.A. Scherer, R.K. Thauer, Purification and properties of reduced ferredoxin: CO_2 oxidoreductase from *Clostridium pasteurianum*, a molybdenum iron–sulfur-protein, Eur. J. Biochem. 85 (1978) 125–135.

[19] S. Mukund, M.W. Adams, Glyceraldehyde-3-phosphate ferredoxin oxidoreductase, a novel tungsten-containing enzyme with a potential glycolytic role in the hyperthermophilic archaeon *Pyrococcus furiosus*, J. Biol. Chem. 270 (1995) 8389–8392.

[20] J.B. Howard, D.C. Rees, Structural basis of biological nitrogen fixation, Chem. Rev. 96 (1996) 2965–2982.

[21] W. Buckel, J. Zhang, P. Friedrich, A. Parthasarathy, H. Li, I. Djurdjevic, H. Dobbek, B.M. Martins, Enzyme catalyzed radical dehydrations of hydroxy acids, Biochim. Biophys. Acta (2011) [online].

[22] M. Boll, G. Fuchs, J. Heider, Anaerobic oxidation of aromatic compounds and hydrocarbons, Curr. Opin. Chem. Biol. 6 (2002) 604–611.

[23] G. Herrmann, E. Jayamani, G. Mai, W. Buckel, Energy conservation via electron-transferring flavoprotein in anaerobic bacteria, J. Bacteriol. 190 (2008) 784–791.

[24] U. Brandt, Bifurcated ubihydroquinone oxidation in the cytochrome bc_1 complex by proton-gated charge transfer, FEBS Lett. 387 (1996) 1–6.

[25] F. Li, J. Hinderberger, H. Seedorf, J. Zhang, W. Buckel, R.K. Thauer, Coupled ferredoxin and crotonyl coenzyme A (CoA) reduction with NADH catalyzed by the butyryl-CoA dehydrogenase/Etf complex from *Clostridium kluyveri*, J. Bacteriol. 190 (2008) 843–850.

[26] G.J. Schut, M.W. Adams, The iron-hydrogenase of *Thermotoga maritima* utilizes ferredoxin and NADH synergistically: a new perspective on anaerobic hydrogen production, J. Bacteriol. 191 (2009) 4451–4457.

[27] S. Wang, H. Huang, J. Moll, R.K. Thauer, $NADP^+$ reduction with reduced ferredoxin and $NADP^+$ reduction with NADH are coupled via an electron-bifurcating enzyme complex in *Clostridium kluyveri*, J. Bacteriol. 192 (2010) 5115–5123.

[28] H. Huang, S. Wang, J. Moll, R.K. Thauer, Electron bifurcation involved in the energy metabolism of the acetogenic bacterium *Moorella thermoacetica* growing on glucose or H_2 plus CO_2, J. Bacteriol. 194 (2012) 3689–3699.

[29] R.K. Thauer, A.K. Kaster, H. Seedorf, W. Buckel, R. Hedderich, Methanogenic archaea: ecologically relevant differences in energy conservation, Nat. Rev. Microbiol. 6 (2008) 579–591.

[30] U. Sauer, F. Canonaco, S. Heri, A. Perrenoud, E. Fischer, The soluble and membrane-bound transhydrogenases UdhA and PntAB have divergent functions in NADPH metabolism of *Escherichia coli*, J. Biol. Chem. 279 (2004) 6613–6619.

[31] R.K. Thauer, K. Jungermann, E. Rupprecht, K. Decker, Hydrogen formation from NADH in cell-free extracts of *Clostridium kluyveri*. Acetyl coenzyme A requirement and ferredoxin dependence, FEBS Lett. 4 (1969) 108–112.

[32] K. Jungermann, E. Rupprecht, C. Ohrloff, R. Thauer, K. Decker, Regulation of the reduced nicotinamide adenine dinucleotide–ferredoxin reductase system in *Clostridium kluyveri*, J. Biol. Chem. 246 (1971) 960–963.

[33] G. Nakos, L. Mortenson, Purification and properties of hydrogenase, an iron sulfur protein, from *Clostridium pasteurianum* W5, Biochim. Biophys. Acta 227 (1971) 576–583.

[34] H. Seedorf, W.F. Fricke, B. Veith, H. Brüggemann, H. Liesegang, A. Strittmatter, M. Miethke, W. Buckel, J. Hinderberger, F. Li, C. Hagemeier, R.K. Thauer, G. Gottschalk, The genome of *Clostridium kluyveri*, a strict anaerobe with unique metabolic features, Proc. Natl. Acad. Sci. U. S. A. 105 (2008) 2128–2133.

[35] C.D. Whitfield, S.G. Mayhew, Purification and properties of electron-transferring flavoprotein from *Peptostreptococcus elsdenii*, J. Biol. Chem. 249 (1974) 2801–2810.

[36] K. Sato, Y. Nishina, K. Shiga, Purification of electron-transferring flavoprotein from *Megasphaera elsdenii* and binding of additional FAD with an unusual absorption spectrum, J. Biochem. 134 (2003) 719–729.

[37] G.E. Herrmann, Enzymes of two clostridial amino-acid fermentation pathways, Philipps-Universität, Marburg, 2008. http://archiv.ub.uni-marburg.de/diss/z2008/0144/pdf/dgeht.pdf.

[38] E. Jayamani, A unique way of energy conservation in glutamate fermenting clostridia, Philipps-Universität, Marburg, 2008. http://archiv.ub.uni-marburg.de/diss/z2009/0712/pdf/dej.pdf.

[39] S. Kölzer, In: Aufreiningung und Charakterisierung des Butyryl-CoA Dehydrogenase/ETF Komplexes aus *Clostridium tetanomorphum*, Fachbereich Biologie, Philipps-Universität, Marburg, 2008, p. 56.

[40] F.L. Crane, H. Beinert, On the mechanism of dehydrogenation of fatty acyl derivatives of coenzyme A. II. The electron-transferring flavoprotein, J. Biol. Chem. 218 (1956) 717–731.

[41] S. Ghisla, C. Thorpe, Acyl-CoA dehydrogenases. A mechanistic overview, Eur. J. Biochem. 271 (2004) 494–508.

[42] D.L. Roberts, F.E. Frerman, J.J. Kim, Three-dimensional structure of human electron transfer flavoprotein to 2.1-A resolution, Proc. Natl. Acad. Sci. U. S. A. 93 (1996) 14355–14360.

[43] R.J. Gorelick, L.M. Schopfer, D.P. Ballou, V. Massey, C. Thorpe, Interflavin oxidation–reduction reactions between pig kidney general acyl-CoA dehydrogenase and electron-transferring flavoprotein, Biochemistry 24 (1985) 6830–6839.

[44] T.M. Dwyer, S. Mortl, K. Kemter, A. Bacher, A. Fauq, F.E. Frerman, The intraflavin hydrogen bond in human electron transfer flavoprotein modulates redox potentials and may participate in electron transfer, Biochemistry 38 (1999) 9735–9745.

[45] D.L. Roberts, D. Salazar, J.P. Fulmer, F.E. Frerman, J.J. Kim, Crystal structure of *Paracoccus denitrificans* electron transfer flavoprotein: structural and electrostatic analysis of a conserved flavin binding domain, Biochemistry 38 (1999) 1977–1989.

[46] W. Buckel, B.T. Golding, Radical enzymes, In: in: C. Chatgilialoglu, A. Studer (Eds.), Handbook of Radicals in Chemistry, Biology and Materials, John Wiley & Sons, Ltd, Chichester, UK, 2012, pp. 1501–1546.

[47] W. Nitschke, M.J. Russell, Redox bifurcations: mechanisms and importance to life now, and at its origin: a widespread means of energy conversion in biology unfolds, Bioessays 34 (2012) 106–109.

[48] M.F. Verhagen, T. O'Rourke, M.W. Adams, The hyperthermophilic bacterium, *Thermotoga maritima*, contains an unusually complex iron-hydrogenase: amino acid sequence analyses versus biochemical characterization, Biochim. Biophys. Acta 1412 (1999) 212–229.

[49] M. Köpke, C. Held, S. Hujer, H. Liesegang, A. Wiezer, A. Wollherr, A. Ehrenreich, W. Liebl, G. Gottschalk, P. Dürre, *Clostridium ljungdahlii* represents a microbial production platform based on syngas, Proc. Natl. Acad. Sci. U. S. A. 107 (2010) 13087–13092.

[50] A. Poehlein, S. Schmidt, A.K. Kaster, M. Goenrich, J. Vollmers, A. Thurmer, J. Bertsch, K. Schuchmann, B. Voigt, M. Hecker, R. Daniel, R.K. Thauer, G. Gottschalk, V. Müller, An ancient pathway combining carbon dioxide fixation with the generation and utilization of a sodium ion gradient for ATP synthesis, PLoS One 7 (2012) e33439.

[51] E. Pierce, G. Xie, R.D. Barabote, E. Saunders, C.S. Han, J.C. Detter, P. Richardson, T.S. Brettin, A. Das, L.G. Ljungdahl, S.W. Ragsdale, The complete genome sequence of *Moorella thermoacetica* (f. *Clostridium thermoaceticum*), Environ. Microbiol. 10 (2008) 2550–2573.

[52] B. Soboh, D. Linder, R. Hedderich, A multisubunit membrane-bound [NiFe] hydrogenase and an NADH-dependent Fe-only hydrogenase in the fermenting bacterium *Thermoanaerobacter tengcongensis*, Microbiology 150 (2004) 2451–2463.

[53] R.K. Thauer, A.K. Kaster, M. Goenrich, M. Schick, T. Hiromoto, S. Shima, Hydrogenases from methanogenic archaea, nickel, a novel cofactor, and H_2 storage, Annu. Rev. Biochem. 79 (2010) 507–536.

[54] T.A. Bobik, R.S. Wolfe, Activation of formylmethanofuran synthesis in cell extracts of *Methanobacterium thermoautotrophicum*, J. Bacteriol. 171 (1989) 1423–1427.

[55] A.K. Kaster, J. Moll, K. Parey, R.K. Thauer, Coupling of ferredoxin and heterodisulfide reduction via electron bifurcation in hydrogenotrophic methanogenic archaea, Proc. Natl. Acad. Sci. U. S. A. 108 (2011) 2981–2986.

[56] A.K. Kaster, M. Goenrich, H. Seedorf, H. Liesegang, A. Wollherr, G. Gottschalk, R.K. Thauer, More than 200 genes required for methane formation from H_2 and CO_2 and energy conservation are present in *Methanothermobacter marburgensis* and *Methanothermobacter thermautotrophicus*, Archaea 2011 (2011) (ID 973848).

[57] R.K. Thauer, E. Rupprecht, C. Ohrloff, K. Jungermann, K. Decker, Regulation of the reduced nicotinamide adenine dinucleotide phosphate–ferredoxin reductase system in *Clostridium kluyveri*, J. Biol. Chem. 246 (1971) 954–959.

[58] B. Buchenau, *Are there tetrahydrofolate specific enzymes in archaea and tetrahydromethanopterin specific enzymes in acetogenic bacteria?* Diploma Thesis, Fachbereich Biologie, Philipps-University, Marburg, 2001.

[59] J.W. Kung, S. Baumann, M. von Bergen, M. Müller, P.L. Hagedoorn, W.R. Hagen, M. Boll, Reversible biological Birch reduction at an extremely low redox potential, J. Am. Chem. Soc. 132 (2010) 9850–9856.

[60] J.W. Kung, C. Löffler, K. Dorner, D. Heintz, S. Gallien, A. Van Dorsselaer, T. Friedrich, M. Boll, Identification and characterization of the tungsten-containing class of benzoyl-coenzyme A reductases, Proc. Natl. Acad. Sci. U. S. A. 106 (2009) 17687–17692.

[61] R.K. Thauer, CO_2 reduction to formate in *Clostridium acidi-urici*, J. Bacteriol. 114 (1973) 443–444.

[62] I.A. Pereira, A.R. Ramos, F. Grein, M.C. Marques, S.M. da Silva, S.S. Venceslau, A comparative genomic analysis of energy metabolism in sulfate reducing bacteria and archaea, Front. Microbiol. 2 (2011) 69.

[63] A.R. Ramos, K.L. Keller, J.D. Wall, I.A. Pereira, The membrane QmoABC complex interacts directly with the dissimilatory adenosine 5′-phosphosulfate reductase in sulfate reducing bacteria, Front. Microbiol. 3 (2012) 137.

[64] P. Mitchell, The protonmotive Q cycle: a general formulation, FEBS Lett. 59 (1975) 137–139.

[65] A. Osyczka, C.C. Moser, P.L. Dutton, Fixing the Q cycle, Trends Biochem. Sci. 30 (2005) 176–182.

[66] J. Zhu, T. Egawa, S.R. Yeh, L. Yu, C.A. Yu, Simultaneous reduction of iron–sulfur protein and cytochrome b(L) during ubiquinol oxidation in cytochrome bc(1) complex, Proc. Natl. Acad. Sci. U. S. A. 104 (2007) 4864–4869.
[67] U. Brandt, G. von Jagow, Analysis of inhibitor binding to the mitochondrial cytochrome c reductase by fluorescence quench titration. Evidence for a 'catalytic switch' at the Q_o center, Eur. J. Biochem. 195 (1991) 163–170.
[68] U. Brandt, B. Trumpower, The protonmotive Q cycle in mitochondria and bacteria, Crit. Rev. Biochem. Mol. Biol. 29 (1994) 165–197.
[69] C.A. Yu, X. Cen, H.W. Ma, Y. Yin, L. Yu, L. Esser, D. Xia, Domain conformational switch of the iron–sulfur protein in cytochrome bc1 complex is induced by the electron transfer from cytochrome bL to bH, Biochim. Biophys. Acta 1777 (2008) 1038–1043.
[70] D. Xia, L. Esser, L. Yu, C.A. Yu, Structural basis for the mechanism of electron bifurcation at the quinol oxidation site of the cytochrome bc_1 complex, Photosynth. Res. 92 (2007) 17–34.
[71] E. Biegel, S. Schmidt, J.M. Gonzalez, V. Müller, Biochemistry, evolution and physiological function of the Rnf complex, a novel ion-motive electron transport complex in prokaryotes, Cell. Mol. Life Sci. 68 (2011) 613–634.
[72] R. Hedderich, L. Forzi, Energy-converting [NiFe] hydrogenases: more than just H_2 activation, J. Mol. Microbiol. Biotechnol. 10 (2005) 92–104.
[73] M. Schmehl, A. Jahn, A. Meyer zu Vilsendorf, S. Hennecke, B. Masepohl, M. Schuppler, M. Marxer, J. Oelze, W. Klipp, Identification of a new class of nitrogen fixation genes in *Rhodobacter capsulatus*: a putative membrane complex involved in electron transport to nitrogenase, Mol. Gen. Genet. 241 (1993) 602–615.
[74] K. Saeki, H. Kumagai, The *rnf* gene products in *Rhodobacter capsulatus* play an essential role in nitrogen fixation during anaerobic DMSO-dependent growth in the dark, Arch. Microbiol. 169 (1998) 464–467.
[75] J. Kim, M. Hetzel, C.D. Boiangiu, W. Buckel, Dehydration of (*R*)-2-hydroxyacyl-CoA to enoyl-CoA in the fermentation of alpha-amino acids by anaerobic bacteria, FEMS Microbiol. Rev. 28 (2004) 455–468.
[76] C.D. Boiangiu, E. Jayamani, D. Brügel, G. Herrmann, J. Kim, L. Forzi, R. Hedderich, I. Vgenopoulou, A.J. Pierik, J. Steuber, W. Buckel, Sodium ion pumps and hydrogen production in glutamate fermenting anaerobic bacteria, J. Mol. Microbiol. Biotechnol. 10 (2005) 105–119.
[77] F. Imkamp, E. Biegel, E. Jayamani, W. Buckel, V. Müller, Dissection of the caffeate respiratory chain in the acetogen *Acetobacterium woodii*: identification of an Rnf-type NADH dehydrogenase as a potential coupling site, J. Bacteriol. 189 (2007) 8145–8153.
[78] M. Hayashi, Y. Nakayama, T. Unemoto, Recent progress in the Na^+-translocating NADH-quinone reductase from the marine *Vibrio alginolyticus*, Biochim. Biophys. Acta 1505 (2001) 37–44.
[79] M. Tao, M.S. Casutt, G. Fritz, J. Steuber, Oxidant-induced formation of a neutral flavosemiquinone in the Na^+-translocating NADH:Quinone oxidoreductase (Na^+-NQR) from *Vibrio cholerae*, Biochim. Biophys. Acta 1777 (2008) 696–702.
[80] M.S. Casutt, T. Huber, R. Brunisholz, M. Tao, G. Fritz, J. Steuber, Localization and function of the membrane-bound riboflavin in the Na^+-translocating NADH: quinone oxidoreductase (Na^+-NQR) from *Vibrio cholerae*, J. Biol. Chem. 285 (2010) 27088–27099.
[81] M.S. Casutt, R. Nedielkov, S. Wendelspiess, S. Vossler, U. Gerken, M. Murai, H. Miyoshi, H.M. Möller, J. Steuber, Localization of ubiquinone-8 in the Na^+-pumping NADH:quinone oxidoreductase from *Vibrio cholerae*, J. Biol. Chem. 286 (2011) 40075–40082.
[82] E. Biegel, V. Müller, Bacterial Na^+-translocating ferredoxin:NAD^+ oxidoreductase, Proc. Natl. Acad. Sci. U. S. A. 107 (2010) 18138–18142.
[83] H. Brüggemann, S. Bäumer, W.F. Fricke, A. Wiezer, H. Liesegang, I. Decker, C. Herzberg, R. Martinez-Arias, R. Merkl, A. Henne, G. Gottschalk, The genome sequence of *Clostridium tetani*, the causative agent of tetanus disease, Proc. Natl. Acad. Sci. U. S. A. 100 (2003) 1316–1321.
[84] O. Juarez, M.E. Shea, G.I. Makhatadze, B. Barquera, The role and specificity of the catalytic and regulatory cation-binding sites of the Na^+-pumping NADH: quinone oxidoreductase from *Vibrio cholerae*, J. Biol. Chem. 286 (2011) 26383–26390.
[85] W. Buckel, Sodium ion-translocating decarboxylases, Biochim. Biophys. Acta 1505 (2001) 15–27.
[86] W. Buckel, R. Semmler, A biotin-dependent sodium pump: glutaconyl-CoA decarboxylase from *Acidaminococcus fermentans*, FEBS Lett. 148 (1982) 35–38.
[87] E. Biegel, V. Müller, A Na^+-translocating pyrophosphatase in the acetogenic bacterium *Acetobacterium woodii*, J. Biol. Chem. 286 (2011) 6080–6084.
[88] C. Welte, C. Krätzer, U. Deppenmeier, Involvement of Ech hydrogenase in energy conservation of *Methanosarcina mazei*, FEBS J. 277 (2010) 3396–3403.
[89] R. Sapra, M.F. Verhagen, M.W. Adams, Purification and characterization of a membrane-bound hydrogenase from the hyperthermophilic archaeon *Pyrococcus furiosus*, J. Bacteriol. 182 (2000) 3423–3428.
[90] R. Sapra, K. Bagramyan, M.W. Adams, A simple energy-conserving system: proton reduction coupled to proton translocation, Proc. Natl. Acad. Sci. U. S. A. 100 (2003) 7545–7550.
[91] I.R. Booth, J.G. Morris, Carbohydrate transport in *Clostridium pasteurianum*, Biosci. Rep. 2 (1982) 47–53.
[92] W.J. Mitchell, J.E. Shaw, L. Andrews, Properties of the glucose phosphotransferase system of *Clostridium acetobutylicum* NCIB 8052, Appl. Environ. Microbiol. 57 (1991) 2534–2539.
[93] J.W. Peters, W.N. Lanzilotta, B.J. Lemon, L.C. Seefeldt, X-ray crystal structure of the Fe-only hydrogenase (CpI) from *Clostridium pasteurianum* to 1.8 angstrom resolution, Science 282 (1998) 1853–1858.
[94] J. Nölling, G. Breton, M.V. Omelchenko, K.S. Makarova, Q. Zeng, R. Gibson, H.M. Lee, J. Dubois, D. Qiu, J. Hitti, Y.I. Wolf, R.L. Tatusov, F. Sabathe, L. Doucette-Stamm, P. Soucaille, M.J. Daly, G.N. Bennett, E.V. Koonin, D.R. Smith, Genome sequence and comparative analysis of the solvent-producing bacterium *Clostridium acetobutylicum*, J. Bacteriol. 183 (2001) 4823–4838.
[95] V. Riebeling, R.K. Thauer, K. Jungermann, The internal-alkaline pH gradient, sensitive to uncoupler and ATPase inhibitor, in growing *Clostridium pasteurianum*, Eur. J. Biochem. 55 (1975) 445–453.
[96] D.J. Clarke, F.M. Fuller, J.G. Morris, The proton-translocating adenosine triphosphatase of the obligately anaerobic bacterium *Clostridium pasteurianum*. 1. ATP phosphohydrolase activity, Eur. J. Biochem. 98 (1979) 597–612.
[97] J.P. Amend, E.L. Shock, Energetics of overall metabolic reactions of thermophilic and hyperthermophilic archaea and bacteria, FEMS Microbiol. Rev. 25 (2001) 175–243.
[98] A.D. Frock, S.R. Gray, R.M. Kelly, Hyperthermophilic *Thermotoga* species differ with respect to specific carbohydrate transporters and glycoside hydrolases, Appl. Environ. Microbiol. 78 (2012) 1978–1986.
[99] M. Selig, K.B. Xavier, H. Santos, P. Schönheit, Comparative analysis of Embden–Meyerhof and Entner–Doudoroff glycolytic pathways in hyperthermophilic archaea and the bacterium *Thermotoga*, Arch. Microbiol. 167 (1997) 217–232.
[100] J. van der Oost, G. Schut, S.W. Kengen, W.R. Hagen, M. Thomm, W.M. de Vos, The ferredoxin-dependent conversion of glyceraldehyde-3-phosphate in the hyperthermophilic archaeon *Pyrococcus furiosus* represents a novel site of glycolytic regulation, J. Biol. Chem. 273 (1998) 28149–28154.
[101] T. Dandekar, S. Schuster, B. Snel, M. Huynen, P. Bork, Pathway alignment: application to the comparative analysis of glycolytic enzymes, Biochem. J. 343 (Pt 1) (1999) 115–124.
[102] K.Y. Pisa, H. Huber, M. Thomm, V. Müller, A sodium ion-dependent A_1A_O ATP synthase from the hyperthermophilic archaeon *Pyrococcus furiosus*, FEBS J. 274 (2007) 3928–3938.
[103] S.J. Lee, M. Surma, W. Hausner, M. Thomm, W. Boos, The role of TrmB and TrmB-like transcriptional regulators for sugar transport and metabolism in the hyperthermophilic archaeon *Pyrococcus furiosus*, Arch. Microbiol. 190 (2008) 247–256.
[104] R.K. Thauer, K. Jungermann, H. Henninger, J. Wenning, K. Decker, The energy metabolism of *Clostridium kluyveri*, Eur. J. Biochem. 4 (1968) 173–180.
[105] W. Buckel, Unusual enzymes involved in five pathways of glutamate fermentation, Appl. Microbiol. Biotechnol. 57 (2001) 263–273.
[106] W. Buckel, H.A. Barker, Two pathways of glutamate fermentation by anaerobic bacteria, J. Bacteriol. 117 (1974) 1248–1260.
[107] R. Reitzer, K. Gruber, G. Jogl, U.G. Wagner, H. Bothe, W. Buckel, C. Kratky, Glutamate mutase from *Clostridium cochlearium*: the structure of a coenzyme B_{12}-dependent enzyme provides new mechanistic insights, Structure 7 (1999) 891–902.
[108] Y.J. Chang, R. Pukall, E. Saunders, A. Lapidus, A. Copeland, M. Nolan, T. Glavina Del Rio, S. Lucas, F. Chen, H. Tice, J.F. Cheng, C. Han, J.C. Detter, D. Bruce, L. Goodwin, S. Pitluck, N. Mikhailova, K. Liolios, A. Pati, N. Ivanova, K. Mavromatis, A. Chen, K. Palaniappan, M. Land, L. Hauser, C.D. Jeffries, T. Brettin, M. Rohde, M. Goker, J. Bristow, J.A. Eisen, V. Markowitz, P. Hugenholtz, N.C. Kyrpides, H.P. Klenk, Complete genome sequence of *Acidaminococcus fermentans* type strain (VR4), Stand Genomic Sci. 3 (2010) 1–14.
[109] U. Härtel, W. Buckel, Sodium ion-dependent hydrogen production in *Acidaminococcus fermentans*, Arch. Microbiol. 166 (1996) 350–356.
[110] C.M. Plugge, J.M. van Leeuwen, T. Hummelen, M. Balk, A.J. Stams, Elucidation of the pathways of catabolic glutamate conversion in three thermophilic anaerobic bacteria, Arch. Microbiol. 176 (2001) 29–36.
[111] A. Braune, K. Bendrat, S. Rospert, W. Buckel, The sodium ion translocating glutaconyl-CoA decarboxylase from *Acidaminococcus fermentans*: cloning and function of the genes forming a second operon, Mol. Microbiol. 31 (1999) 473–487.
[112] G. Gottschalk, R.K. Thauer, The Na^+-translocating methyltransferase complex from methanogenic archaea, Biochim. Biophys. Acta 1505 (2001) 28–36.
[113] U. Deppenmeier, V. Müller, Life close to the thermodynamic limit: how methanogenic archaea conserve energy, Results Probl. Cell Differ. 45 (2008) 123–152.
[114] M. Hetzel, M. Brock, T. Selmer, A.J. Pierik, B.T. Golding, W. Buckel, Acryloyl-CoA reductase from *Clostridium propionicum*. An enzyme complex of propionyl-CoA dehydrogenase and electron-transferring flavoprotein, Eur. J. Biochem. 270 (2003) 902–910.
[115] R.L. Baldwin, L.P. Milligan, Electron transport in *Peptostreptococcus elsdenii*, Biochim. Biophys. Acta 92 (1964) 421–432.
[116] S. Seeliger, P.H. Janssen, B. Schink, Energetics and kinetics of lactate fermentation to acetate and propionate via methylmalonyl-CoA or acrylyl-CoA, FEMS Microbiol. Lett. 211 (2002) 65–70.
[117] W. Lehnert, J.O. Sass, Glutaconyl-CoA is the main toxic agent in glutaryl-CoA dehydrogenase deficiency (glutaric aciduria type I), Med. Hypotheses 65 (2005) 330–333.
[118] L. Shaw, P.C. Engel, The suicide inactivation of ox liver short-chain acyl-CoA dehydrogenase by propionyl-CoA. Formation of an FAD adduct, Biochem. J. 230 (1985) 723–731.
[119] J. Simon, R.J. van Spanning, D.J. Richardson, The organisation of proton motive and non-proton motive redox loops in prokaryotic respiratory systems, Biochim. Biophys. Acta 1777 (2008) 1480–1490.
[120] W. Nitschke, M.J. Russell, Hydrothermal focusing of chemical and chemiosmotic energy, supported by delivery of catalytic Fe, Ni, Mo/W, Co, S and Se, forced life to emerge, J. Mol. Evol. 69 (2009) 481–496.

[121] W.F. Martin, Hydrogen, metals, bifurcating electrons, and proton gradients: the early evolution of biological energy conservation, FEBS Lett. 586 (2012) 485–493.
[122] R. Banerjee, S.W. Ragsdale, The many faces of vitamin B_{12}: catalysis by cobalamin-dependent enzymes, Annu. Rev. Biochem. 72 (2003) 209–247.
[123] H. Smidt, W.M. de Vos, Anaerobic microbial dehalogenation, Annu. Rev. Microbiol. 58 (2004) 43–73.
[124] T. Futagami, M. Goto, K. Furukawa, Biochemical and genetic bases of dehalorespiration, Chem. Rec. 8 (2008) 1–12.
[125] J. Maillard, M.P. Charnay, C. Regeard, E. Rohrbach-Brandt, K. Rouzeau-Szynalski, P. Rossi, C. Holliger, Reductive dechlorination of tetrachloroethene by a stepwise catalysis of different organohalide respiring bacteria and reductive dehalogenases, Biodegradation 22 (2011) 949–960.